
Addressing Mark Imbalance in Integration-free Neural Marked Temporal Point Processes

Sishun Liu
 RMIT University
 Melbourne, Victoria 3000
 sishun.liu@student.rmit.edu.au

Ke Deng
 RMIT University
 Melbourne, Victoria 3000
 ke.deng@rmit.edu.au

Yongli Ren
 RMIT University
 Melbourne, Victoria 3000
 yongli.ren@rmit.edu.au

Yan Wang
 Macquarie University
 Sydney, New South Wales 2000
 yan.wang@mq.edu.au

Xiuzhen Zhang
 RMIT University
 Melbourne, Victoria 3000
 xiuzhen.zhang@rmit.edu.au

Abstract

Marked Temporal Point Process (MTPP) has been well studied to model the event distribution in marked event streams, which can be used to predict the mark and arrival time of the next event. However, existing studies overlook that the distribution of event marks is highly imbalanced in many real-world applications, with some marks being frequent but others rare. The imbalance poses a significant challenge to the performance of the next event prediction, especially for events of rare marks. To address this issue, we propose a *thresholding* method, which learns thresholds to tune the mark probability normalized by the mark’s prior probability to optimize mark prediction, rather than predicting the mark directly based on the mark probability as in existing studies. In conjunction with this method, we predict the mark first and then the time. In particular, we develop a novel neural MTPP model to support effective time sampling and estimation of mark probability without computationally expensive numerical improper integration. Extensive experiments on real-world datasets demonstrate the superior performance of our solution against various baselines for the next event mark and time prediction. The code is available at <https://github.com/undesired/IFNMTPP>.

1 Introduction

Marked Temporal Point Process (MTPP) models event sequences observed from natural phenomena (e.g. earthquakes) or generated in human activities (e.g. retweets), where each event has a mark and an arrival time. MTPP has attracted the attention of the research community (see Shchur et al. [34] for a comprehensive review). Typically, MTPP models the joint *Probability Distribution Function (PDF)* conditioned on history, denoted as $p^*(m, t)$ ¹, where m and t are the mark and arrival time² of the next event, respectively. Some studies are on the Poisson Process [37] and Hawkes process

¹The asterisk reminds the probability is conditioned on history, i.e., the events in the past.

²The time relative to the most recent event

[32, 16, 27]. Recently, we have witnessed a rapid growth of *neural MTPP*, which models $p^*(m, t)$ using neural networks [24, 28, 41, 26, 43], due to the capability of learning complicated temporal patterns and computational efficiency [34].

However, existing studies overlook that the distribution of event marks is highly imbalanced in many real-world applications, with some marks being frequent but others rare, as shown in Figure 1 (a). Similar to other machine learning tasks such as classification, the imbalance poses a significant challenge to the performance of the next event prediction, especially for events of rare marks, which are often more important than other marks (e.g., the occurrence of a 7-magnitude earthquake or a retweet from celebrities). By mitigating the impact of mark imbalance, this study aims to improve the performance of MTPP for next event prediction.

Various techniques have been investigated to improve prediction performance for rare classes in classifiers, including *resampling the training set*, *cost-sensitive approaches*, and *thresholding* [17, 1, 39]. Training data resampling requires a proper resampling ratio. Cost-sensitive approaches requires domain knowledge regarding the importance of different marks to set the cost [17]. To have a solution with minimum external knowledge and assumptions, this study adopts thresholding, which learns thresholds to tune the mark probability normalized by the prior probability of marks.

Addressing mark imbalance for MTPP using thresholding is not straightforward. In addition to mark prediction, MTPP also needs to predict the time simultaneously. In most existing MTPP studies, the strategy is to predict the time based on $p^*(t)$, the probability that the next event time is t , and then predict the mark based on $p^*(m|t)$, the probability that the next event mark is m at the predicted time t . Our analysis and experiments show that this strategy is unsuitable for addressing mark imbalance with thresholding. If time changes, the mark probability conditioned on time typically changes and thus requires different tuning thresholds. However, it is implausible to learn the tuning thresholds at all times. So, we propose a strategy that first predicts the mark based on $p^*(m)$, the probability that the next event mark is m , and then predicts the time based on $p^*(t|m)$, the probability that the next event time is t on the condition that the predicted mark m is the next event mark. Since the mark probability $p^*(m)$ is independent of time, it is easy to apply thresholding to handle mark imbalance.

However, our strategy has its challenges. First, two different improper integrations are required for modeling $p^*(m)$ and time prediction, respectively. Second, sampling $p^*(t|m)$ to predict time is inefficient because it needs the *Cumulative Distribution Function (CDF)* of $p^*(t|m)$, but the CDF does not have a closed-form expression. To overcome these challenges, we find a way to unify the two improper integrations into one. Then, we develop a novel MTPP model, called *Integration-free Neural Marked Temporal Point Process (IFNMTPP)*, to approximate the unified improper integration, rather than using a computationally expensive numerical method. With IFNMTPP, we can directly model $p^*(m)$ and the CDF of $p^*(t|m)$. The CDF makes drawing samples from $p^*(t|m)$ efficient for time prediction. Based on $p^*(m)$, the thresholding method can be applied to address the mark imbalance. Extensive experiments on real-world datasets demonstrate the superior performance of our solution against various baselines for the next event mark and time prediction. The contributions of this study are threefold:

- This study investigates the impact of mark imbalance on MTPP for next event prediction, which is overlooked by existing MTPP studies.
- This study introduces the first solution to address mark imbalance in MTPP, which learns thresholds to tune the mark probability normalized by the prior probability of marks to optimize mark prediction, rather than predicting mark based on mark probability directly as in existing studies.
- This study finds a way to unify two improper integrations into one, and proposes a novel *Integration-free Neural Marked Temporal Point Process (IFNMTPP)* to approximate the unified improper integration to support time sampling and estimation of mark probability, rather than using computationally expensive numerical improper integration.

2 Preliminaries

2.1 Marked Temporal Point Process

The Marked Temporal Point Process (MTPP) is a random process whose embodiment is a sequence of discrete events, $\mathcal{S} = \{(m_i, t_i)\}_{i=1}^n$, where $i \in \mathbb{Z}^+$ is the sequence order, $t_i \in \mathbb{R}^+$ is the time

when the i th event occurs, m_i is the mark of the i th event. This study only concerns a finite set of categorical marks $M = \{k_1, k_2, \dots, k_{|M|}\}$, and the simple MTPP, which allows at most one event at every time, thus $t_i < t_j$ if $i < j$. The time of the most recent event is t_l , and the current time is $t > t_l$. The time interval between two adjacent events is the inter-event time. We assume that an event with a particular mark at a particular time may be triggered by past events. Let \mathcal{H}_{t_l} be the history up to (including) the most recent event, and \mathcal{H}_{t-} be the history up to (excluding) the current time [31]. With these definitions, we can define the *Conditional Intensity Function (CIF)* of MTPP:

$$\lambda^*(m = k_i, t) = \lambda(m = k_i, t | \mathcal{H}_{t-}) = \lim_{\Delta t \rightarrow 0} \frac{P(m = k_i, t \in [t, t + \Delta t) | \mathcal{H}_{t-})}{\Delta t}. \quad (1)$$

With $\lambda^*(m, t)$, the conditional joint PDF of the next event can be defined:

$$p^*(m, t) = p(m, t | \mathcal{H}_{t_l}) = \lambda^*(m, t) F^*(t) = \lambda^*(m, t) \exp\left(-\int_{t_l}^t \sum_{n \in M} \lambda^*(n, \tau) d\tau\right). \quad (2)$$

where τ means integrating over time. $F^*(t)$ is the conditional PDF that no event has ever happened up to time t since t_l . We explain how to obtain Equation (2) from Equation (1) in Section A.

The simplest form of MTPP is the homogeneous Poisson process whose CIF merely contains a positive number, i.e., $\lambda^*(m = k_i, t) = c$. Another example is the Hawkes process [14], belonging to the self-exciting point process family. Its CIF is $\lambda^*(m = k_i, t) = \mu_i + \sum_{j: t_j < t} \kappa_i(t, t_j)$ where $\kappa_i(t, t_j) > 0$ represents the excite from previous events. Because it meets the real-world intuition that the influences of occurred events always drastically drops as time passes, the Hawkes process is a widely used backbone process in various models [4, 27, 16, 15]. Recently, we have witnessed a rapid growth of neural MTPP, which models $p^*(m, t)$ using neural networks [24, 28, 41, 26, 43], due to the capability of learning complicated temporal patterns and computational efficiency [34].

Based on $p^*(m, t)$, the mark m and time t of the next event can be predicted. Most existing MTPP methods predict when the next event will occur first, and then predict what the mark is at the predicted time. Specifically, the expected time of the next event is $\bar{t} = \int_{t=t_l}^{\infty} \tau p^*(\tau) d\tau$ where $p^*(t) = \sum_{m \in M} p^*(m, t)$. A numerical method is typically used to calculate \bar{t} by sampling N times, denoted as $\{t^i\}_N$, from $p^*(t)$ following *Thinning Algorithm (TA)* or *Inverse Transform Sampling (ITS)* [31] so that $\bar{t} = \frac{1}{N} \sum_i t^i$. After that, the mark of the next event at \bar{t} is predicted: $m_{\bar{t}} = \arg \max_{m \in M} p^*(m, \bar{t})$. Some studies predict the mark of the next event $m = \arg \max_{m \in M} p^*(m)$ and then predict the time of the next event $\bar{t}_m = \int_{t=t_l}^{\infty} \tau p^*(\tau | m) d\tau$ given the predicted mark [36].

2.2 Mark Imbalance

In real-world scenarios, the mark distribution can be significantly imbalanced, i.e., some marks are persistent and others are rare. The imbalance hurts the performance of the next event prediction, especially for rare marks, which are often more important than other marks (e.g., the occurrence of a 7-magnitude earthquake). Let us consider two marks k_1 and k_2 where k_1 is much more frequent than k_2 in the observed event sequence. Suppose the next event is mark k_2 . Because k_1 is much more frequent than k_2 , it is very likely that $p^*(k_1, t) > p^*(k_2, t)$ for most of the time t , including $\bar{t} = \int_{t=t_l}^{\infty} \tau \sum_{m \in M} p^*(m, \tau) d\tau$. If so, k_1 will be predicted as the next event, but the real mark is k_2 .

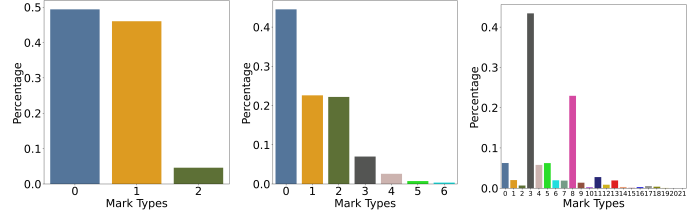
Figure 1 (a) demonstrates the mark frequency distribution in three datasets, Retweet, USearquake, and StackOverflow (see details in Section 4). Figure 1 (b) shows $p^*(m, t)$ for each mark m in these datasets. The envelope covers $p^*(m, t)$ of all instances in the datasets, and the line is the average of $p^*(m, t)$ across these instances. These figures show that $p^*(k_1, t) > p^*(k_2, t)$ for most of the time if k_1 is frequent and k_2 is rare. Table 1 shows the mark prediction performance achieved by SAHP [41], a neural MTPP model, on rare and frequent marks, respectively, measured by macro-F1. We can see that the prediction performance for rare marks is significantly lower than that for frequent marks.

3 Methodology

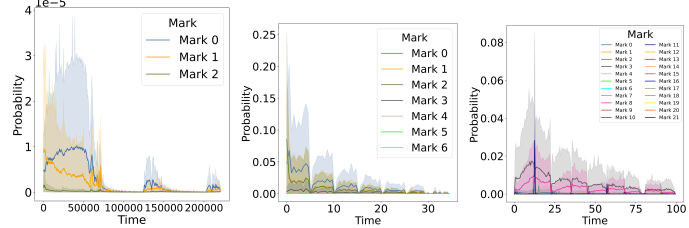
To improve the performance of MTPP for next event prediction, this study handles mark imbalance with a thresholding method, which learns thresholds to tune the mark probability normalized by the

Table 1: Mark prediction performance measured by macro-F1 using SAHP [41] for rare and frequent marks on three real-world datasets.

Retweet	Rare Marks	0.0266 ± 0.0135
	Freq Marks	0.6183 ± 0.0010
USearquake	Rare Marks	0.0037 ± 0.0010
	Freq Marks	0.2196 ± 0.0016
StackOverflow	Rare Marks	0.0863 ± 0.0032
	Freq Marks	0.2054 ± 0.0011



(a) The frequency distribution of marks in Retweet, USearquake, and StackOverflow (from left to right).



(b) The $p^*(m, t)$ for each mark m in Retweet, USearquake, and StackOverflow (from left to right).

Figure 1: A demonstration of the mark imbalance in various datasets and its influence on $p^*(m, t)$.

mark’s prior probability to optimize mark prediction. In conjunction with the thresholding method, the proposed method predicts the mark based on $p^*(m)$ and then, given the predicted mark m , predicts the time based on $p^*(t|m)$.

3.1 Next Event Mark Prediction with Thresholding

The mark prediction of the next event depends on accurately modeling $p^*(m)$ for each mark m , the probability that the mark of the next event is m , based on $p^*(m, t)$. The expression of $p^*(m)$ is:

$$p^*(m) = \int_{t_i}^{+\infty} p^*(m, \tau) d\tau \quad (3)$$

In general, the frequent mark has a high $p^*(m)$ and the rare mark has a low $p^*(m)$. Inspired by the thresholding method [19, 7], we normalize the probability for each mark by its prior probability and learn to tune it to improve the prediction performance for rare marks. Specifically, for mark m , we calculate the ratio between the probability of m , $p^*(m)$, and its prior probability, $\bar{p}^*(m)$:

$$r_m = \frac{p^*(m)}{\bar{p}^*(m)} \quad (4)$$

In this paper, $\bar{p}^*(m)$ is the proportion of mark m in the training set. $p^*(m)$ measures the probability that the next event mark is m . If m is more frequent than m' , $p^*(m)$ is expected to be higher than $p^*(m')$. In contrast, r_m evaluates whether $p^*(m)$ is higher relative to its own proportion. A rare mark having a low $p^*(m)$ may have a high r_m to signal a high chance of being the next event mark. In this way, the chance of rare marks in the next event prediction is rectified.

With r_m for every mark m , the next event mark prediction m_p is obtained by a thresholding method:

$$m_p = \arg \max_m (r_m - \epsilon_m) \quad (5)$$

where ϵ_m is the threshold of r_m . We learn ϵ_m , which maximizes the accuracy of m_p on the training set. Specifically, for each mark m , if we predict the next mark as m when $r_m > \epsilon_m$ and not m when $r_m \leq \epsilon_m$, the learned ϵ_m maximizes the F1 score of the pairwise comparison, i.e., mark m vs. all other marks. The technical details of the thresholding method are in Section C.2.

3.2 Next Event Time Prediction

After mark prediction, we predict the time. Let $p^*(t|m)$ be the PDF of the next event time on the condition that the next event mark is m . Based on $p^*(t|m)$, we have:

$$\bar{t}_m = \mathbb{E}_{t \sim p^*(\tau|m)}[t] = \int_{t_l}^{+\infty} \tau p^*(\tau|m) d\tau \quad (6)$$

where \bar{t}_m is the expected time of the next event given the mark m .

3.3 Unifying Integral Functions

By the definition in Equation (3) and Equation (6), we must solve the improper integration of $p^*(m, \tau)$ and $\tau p^*(\tau|m)$ for mark probability $p^*(m)$ and time prediction \bar{t} , respectively. In general, improper integration does not have analytic solutions. This means that directly calculating $p^*(m)$ and \bar{t}_m following Equation (3) and Equation (6) is impossible. The solution is to approximate $p^*(m)$ and \bar{t} . In particular, \bar{t} is approximated as the average of N samples $\{t^i\}_N^m$ from $p^*(t|m)$ as Equation (7).

$$\bar{t}_m = \mathbb{E}_{t \sim p^*(\tau|m)}[t] \approx \frac{1}{N} \sum_{i=1}^N t^i \quad (7)$$

To draw $\{t^i\}_N^m$ from $p^*(t|m)$, we use Inverse Transform Sampling (ITS), which takes the Cumulative Distribution Function (CDF) of the distribution that one wants to sample from. In our case, let $F^*(t|m)$ be the CDF of $p^*(t|m)$, i.e., $F^*(t|m) = \int_{t_l}^t p^*(\tau|m) d\tau$. $F^*(t|m)$ refers to the probability of the next event happening in $(t_l, t]$ on the condition that its mark is m . To draw a sample t^i from $p^*(t|m)$, we need to solve Equation (8).

$$F^*(t^i|m) = u^i \quad (8)$$

where u^i is a random sample from a uniform distribution $U(0, 1)$. Since $F^*(t|m)$ is monotonic, Equation (8) is solvable by the bisection method. For each mark m , we obtain $\{t^i\}_N^m$ by solving Equation (8) N times, which allows acquiring an arbitrary number of samples for time prediction no matter rare or frequent the mark m is. We can express $F^*(t|m)$ as follows:

$$F^*(t|m) = \frac{F^*(m, t)}{p^*(m)} = \frac{1}{\int_{t_l}^{+\infty} p^*(m, \tau) d\tau} \int_{t_l}^t p^*(m, \tau) d\tau \quad (9)$$

where $p^*(m) = \int_{t_l}^{+\infty} p^*(m, \tau) d\tau$ is the probability that the mark of next event is m since t_l , and $F^*(m, t) = \int_{t_l}^t p^*(m, \tau) d\tau$ is the probability that the next event is mark m and happens in time interval $(t_l, t]$. We can further breakdown $F^*(m, t)$ as shown in Equation (10).

$$F^*(m, t) = \int_{t_l}^t p^*(m, \tau) d\tau = \int_{t_l}^{+\infty} p^*(m, \tau) d\tau - \int_t^{+\infty} p^*(m, \tau) d\tau \quad (10)$$

For each mark $m \in M$, we define $\Gamma^*(m, t)$ as the integration starting from time t , any time after t_l or t_l , to positive infinity:

$$\Gamma^*(m, t) = \int_t^{+\infty} p^*(m, \tau) d\tau \quad (11)$$

$\Gamma^*(m, t)$ is monotonically decreasing as its derivative $-p^*(m, t)$ is always smaller than 0. We rewrite $p^*(m)$ in Equation (3) and $F^*(t|m)$ in Equation (9) using $\Gamma^*(m, t)$:

$$p^*(m) = \Gamma^*(m, t_l) \quad (12)$$

$$F^*(t|m) = \frac{\Gamma^*(m, t_l) - \Gamma^*(m, t)}{\Gamma^*(m, t_l)} \quad (13)$$

This means two improper integrations in Equation (3) and Equation (6) are now unified into one, i.e., $\Gamma^*(m, t)$, for modeling $p^*(m)$ and time prediction.

While drawing samples from a distribution can follow Thinning Algorithm (TA) or Inverse Transform Sampling (ITS) [31], only ITS is suitable for integral function unification here. The basic idea in ITS is to simulate using CDF of $p^*(t|m)$. Instead, Thinning Algorithm (TA) explicitly requires the expression of $p^*(t|m)$, which is unknown typically.

3.4 Integration-free Neural Marked Temporal Point Process (IFNMTPP)

With $\Gamma^*(m, t)$, we can model $p^*(m)$ and prediction time \bar{t}_m . However, $\Gamma^*(m, t)$ is an improper integral with an infinite integration interval. Numerical methods are computationally expensive and can only be used to estimate integrals on a finite interval. To avoid numerical methods, we introduce Integration-free Neural Marked Temporal Point Process (IFNMTPP) to approximate $\Gamma^*(m, t)$. For each mark m , IFNMTPP models the relationship between $p^*(m, t)$ and its integral $\Gamma^*(m, t)$.

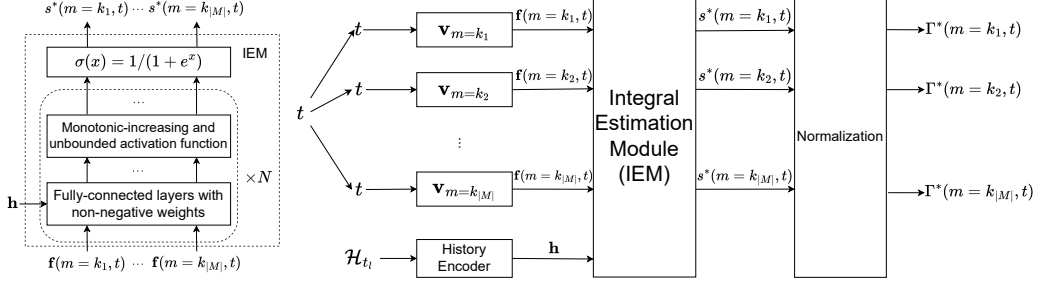


Figure 2: Architecture of IFNMTPP where the history encoder is an LSTM.

Figure 2 sketches the architecture of IFNMTPP. For each mark $m \in M$, we assign a vector \mathbf{v}_m to prepare $\mathbf{f}(m, t) = \mathbf{v}_m(t - t_l) + \mathbf{b}_m$ as input of the Integral Estimation Module (IEM). All parameters in \mathbf{v}_m are non-negative. IEM contains multiple fully-connected layers with non-negative weights, and monotonic-increasing and unbounded activation functions. Then, it ends with a monotonically decreasing function $\sigma(x) = 1/(1 + e^x)$. So, IFNMTPP is intrinsically monotonically decreasing w.r.t. t . The outputs of IEM are scores $s^*(m = k_1, t), s^*(m = k_2, t), \dots, s^*(m = k_{|M|}, t)$. The value of $\sum_{m \in M} s^*(m, t)$ is not guaranteed to be 1. To produce the qualified probability distribution, they need to be normalized. This is achieved by the Normalization module in Figure 2 that divides $s^*(m, t)$ by the partition function $Z(\mathcal{H}_{t_l}) = \sum_{m \in M} s^*(m, t_l)$ for each $m \in M$. Finally, IFNMTPP outputs $\Gamma^*(m, t)$ for each mark m at the given time t :

$$\Gamma^*(m, t) = \frac{s^*(m, t)}{Z(\mathcal{H}_{t_l})} \quad (14)$$

With $\Gamma^*(m, t)$ and $\Gamma^*(m, t_l)$, we have $F^*(t|m)$ by Equation (9) and Equation (10). Next, we calculate \bar{t}_m by drawing $\{t^i\}_N^m$ from $F^*(t|m)$ following Equation (8). With the definition of IFNMTPP, we have the following proposition, with the proof in Section B, to guarantee that the model output is $\Gamma^*(m, t)$:

Proposition 3.1. *The output of IFNMTPP is $\Gamma^*(m, t)$ when its gradient is $-p^*(m, t)$.*

We train IFNMTPP using the Negative Log-Likelihood (NLL) on event sequence \mathcal{S} observed in a time interval $[t_0, T]$, where the time of the first event is $t_1 \geq t_0$, and the time of the last event is $t_s \leq T$.

$$\begin{aligned} L &= -\log p(\mathcal{S}) = -\sum_{(m_i, t_i) \in \mathcal{S}} \log \lambda^*(m_i, t_i) + \int_{t_0}^T \sum_{n \in M} \lambda^*(n, \tau) d\tau \\ &= -\sum_{(m_i, t_i) \in \mathcal{S}} (\log \lambda^*(m_i, t_i) - \int_{t_{i-1}}^{t_i} \sum_{n \in M} \lambda^*(n, \tau) d\tau) + \int_{t_s}^T \sum_{n \in M} \lambda^*(n, \tau) d\tau \\ &= -\sum_{(m_i, t_i) \in \mathcal{S}} \log p^*(m_i, t_i) - \log(1 - \sum_{n \in M} F^*(n, T)) \\ &= -\sum_{(m_i, t_i) \in \mathcal{S}} \log p^*(m_i, t_i) - \log(\sum_{n \in M} \Gamma^*(n, T)) \end{aligned} \quad (15)$$

where $p^*(m_i, t_i)$ is the probability of the i th event conditioned on historical events. IFNMTPP increases $p^*(m_i, t_i)$ where $(m_i, t_i) \in \mathcal{S}$ are real events in event sequences. The term

Table 2: Mark prediction performance measured by macro-F1/micro-F1 to evaluate thresholding and the prediction order of mark and time. The bold are the best values.

		Retweet	SO	Taobao	USearquake
ours	M	0.4750 \pm 0.0033/ 0.4394 \pm 0.0093	0.1776 \pm 0.0030/ 0.6376 \pm 0.0026	0.4190 \pm 0.0104/ 0.7499 \pm 0.0151	0.1382 \pm 0.0071/ 0.3189 \pm 0.0125
	M _r	0.2010 \pm 0.0082/ 0.2010 \pm 0.0082	0.1476 \pm 0.0041/ 0.4530 \pm 0.0026	0.3987 \pm 0.0108/ 0.7558 \pm 0.0185	0.0339 \pm 0.0051/ 0.1111 \pm 0.0098
	M _f	0.6120 \pm 0.0013/0.9612 \pm 0.0021	0.2795 \pm 0.0014/0.8974 \pm 0.0042	0.7441 \pm 0.0060/ 0.7441 \pm 0.0060	0.2773 \pm 0.0215/0.9181 \pm 0.0102
time-mark-with-thresholding	M	0.4741 \pm 0.0028/0.4380 \pm 0.0016	0.1431 \pm 0.0075/0.5834 \pm 0.0028	0.3289 \pm 0.0193/0.7059 \pm 0.0384	0.1214 \pm 0.0126/0.3091 \pm 0.0083
	M _r	0.2000 \pm 0.0067/0.2000 \pm 0.0011	0.1023 \pm 0.0094/0.3829 \pm 0.0044	0.3054 \pm 0.0201/0.7072 \pm 0.0690	0.0298 \pm 0.0093/0.1049 \pm 0.0059
	M _f	0.6093 \pm 0.0008/0.9596 \pm 0.0019	0.2815 \pm 0.0022/0.8888 \pm 0.0041	0.7062 \pm 0.0204/0.7062 \pm 0.0204	0.2436 \pm 0.0236/0.9116 \pm 0.0064
ours-w/o-thresholding	M	0.4269 \pm 0.0010/0.1800 \pm 0.0093	0.1287 \pm 0.0031/0.5877 \pm 0.0023	0.3968 \pm 0.0138/0.7183 \pm 0.0220	0.1153 \pm 0.0061/0.1172 \pm 0.0048
	M _r	0.0333 \pm 0.0082/0.0333 \pm 0.0034	0.1065 \pm 0.0047/0.3763 \pm 0.0030	0.3759 \pm 0.0150/0.7059 \pm 0.0332	0.0121 \pm 0.0035/0.0146 \pm 0.0012
	M _f	0.6238 \pm 0.0001/ 0.9770 \pm 0.0000	0.2043 \pm 0.0022/ 0.9180 \pm 0.0004	0.7311 \pm 0.0108/0.7311 \pm 0.0108	0.2528 \pm 0.0118/ 0.9451 \pm 0.0005
time-mark-w/o-thresholding	M	0.4252 \pm 0.0033/0.1815 \pm 0.0077	0.0906 \pm 0.0055/0.4428 \pm 0.0080	0.3135 \pm 0.0136/0.6384 \pm 0.0116	0.1066 \pm 0.0040/0.1111 \pm 0.0336
	M _r	0.0338 \pm 0.0029/0.0338 \pm 0.0029	0.0567 \pm 0.0071/0.2142 \pm 0.0076	0.2897 \pm 0.0137/0.5884 \pm 0.0467	0.0033 \pm 0.0024/0.0143 \pm 0.0092
	M _f	0.6208 \pm 0.0008/ 0.9770 \pm 0.0001	0.2059 \pm 0.0004/0.9156 \pm 0.0013	0.6933 \pm 0.0129/0.6933 \pm 0.0129	0.2444 \pm 0.0085/0.9446 \pm 0.0002

$\log(\sum_{m \in M} \Gamma^*(m, T))$ is the survival term, which models no events after the last event t_s in each event sequence until time T . In IFNMTPP, the expression of $p^*(m_i, t_i)$ is:

$$p^*(m_i, t_i) = -\frac{\partial \Gamma^*(m_i, t_i)}{\partial t_i} = -\frac{1}{Z(\mathcal{H}_{t_i})} \frac{\partial s^*(m_i, t_i)}{\partial \mathbf{f}(m_i, t_i)} \frac{\partial \mathbf{f}(m_i, t_i)}{\partial t_i} \quad (16)$$

Mei et al. [25] prove that an MTPP model converges to the true distribution when trained with the NLL loss defined in Equation (15). Combined with Theorem 3.1, IFNMTPP consistently estimates the true value of $\Gamma^*(m, t)$.

4 Experiments

We run every experiment 5 times with different random seeds and report the mean and standard deviation (1-sigma) of all results. The complete experiment settings are described in Section D.

Datasets³ Four real-world datasets include Retweet [42], StackOverflow(SO) [20], Taobao User Behavior Data(Taobao) [2], and earthquake events over the Conterminous US(USearquake) [38]. We split all marks of each dataset into two subsets, one containing frequent marks, denoted as M_f, the other containing rare marks, denoted as M_r. M_r \cap M_f = \emptyset and M_r \cup M_f = M. The rare marks and frequent marks for each dataset are described in Section D.5.

Baseline Models⁴ Our method, denoted as *ours*, uses IFNMTPP for predicting the mark of the next event, optimized with thresholding, then uses IFNMTPP to predict the time of the next event given the predicted mark. The first group of baselines includes: (i) *ours-w/o-thresholding* to evaluate the effectiveness of the thresholding method. (ii) *time-mark-with-thresholding* to evaluate the necessity to predict mark first for handling mark imbalance with thresholding. (iii) *time-mark-w/o-thresholding* same as time-mark-with-thresholding but mark prediction is not optimized with thresholding. The second group of baselines evaluates thresholding against resampling, another classic technique to address data imbalance, including *undersampling* and *oversampling*. The third group of baselines includes existing MTPP methods. Since MTPP modeling has been well studied in the past decades, the state-of-the-art methods demonstrate comparable performance. Among them, this study selects the most popular ones as baselines, including FullyNN [28], THP [44], SAHP [41], AttNHP [26], and Marked-LNM [36]. The details of these baselines are available in Section D.4.

Evaluation Metrics We use macro-F1 and micro-F1, described in Section D.3.2, to evaluate mark predictions and use Mean Absolute Error (MAE), described in Section D.3.3, to evaluate time predictions on real-world datasets. The evaluation metrics for mark and time are independent of each other. For each dataset, as discussed above, three sets M, M_f, and M_r are drawn from the original test set. Moreover, we evaluate the fidelity of IFNMTPP using five synthetic datasets. Experiment results on synthetic datasets (reported in Section E.2) demonstrate the high fidelity of IFNMTPP compared with other MTPP models.

³Retweet, StackOverflow, Taobao, and USearquake are released under Apache-2.0 license[38].

⁴Our codes will be released under MIT license.

4.1 Experiment results

Impact of Thresholding on Mark Prediction For the mark prediction, we evaluate (i) the effectiveness of the proposed thresholding method by comparing *ours* with *ours-w/o-thresholding*, (ii) the necessity of the strategy to predict the mark first by comparing *ours* with *time-mark-with-thresholding*. The metric is macro-F1 and micro-F1, where the higher values indicate more accurate mark predictions. The experimental results are reported in Table 2. Compared with *ours-w/o-thresholding*, *ours* has a much better performance on rare mark prediction and a better performance on all mark prediction. *ours* also shows a comparable performance on frequent mark prediction. It implies that the recall of frequent mark prediction is improved using thresholding.

In Table 2, the performance of *ours* is better than *time-mark-with-thresholding* on rare mark prediction on all datasets. To check whether the suboptimal performance of *time-mark-with-thresholding* is due to applying thresholding or not, we also compare *time-mark-with-thresholding* with *time-mark-w/o-thresholding*. The experimental results show that the performance of *time-mark-w/o-thresholding* is lower than that of *time-mark-with-thresholding*. This indicates that predicting the mark first is more suitable for handling mark imbalance with thresholding.

Time Prediction Performance For time prediction performance evaluation, we compare the time predicted using *ours*, i.e., based on $p^*(t|m)$, and that using *time-mark-with-thresholding*, i.e., based on $p^*(t)$. The metric is MAE. Lower MAE means better. The experimental results are reported in Table 3. We observe that predicting time based on $p^*(t|m)$ slightly outperforms that based on $p^*(t)$. The results indicate that the strategy to predict the mark first and then time also benefits the time prediction. The reason could be that \bar{t}_m obtained by drawing samples from $p^*(t|m)$ is more specific to the mark and thus tends to be more accurate compared to \bar{t} obtained based on $p^*(t)$ for all marks.

Thresholding vs. Resampling We compare the prediction performance of *ours* against resampling baselines *oversampling* and *undersampling*. As discussed in Section 1, *resampling the training set* and *cost-sensitive approaches* are two commonly used for handling data imbalance besides *thresholding*. According to López et al. [22], *resampling the training set* and *cost-sensitive approaches* are statistically equivalent. So, we focus on *resampling the training set* only. The experiment results are reported in Table 5. We observe that *ours* consistently outperforms *oversampling* and *undersampling*. It is easy to see that the resampling ratio impacts the performance, but it is hard to figure out the right ratio for different marks on different datasets.

Table 5: Mark prediction performance to evaluate thresholding and resampling, measured by macro-F1/micro-F1, The bold are the best values.

		Retweet	SO	Taobao	USearhquake
ours	M	0.4750 \pm 0.0033/0.4394 \pm 0.0093	0.1776 \pm 0.0030/0.6376 \pm 0.0026	0.4190 \pm 0.0104/0.7499 \pm 0.0151	0.1382 \pm 0.0071/0.3189 \pm 0.0125
	M_r	0.2010 \pm 0.0082/0.2010 \pm 0.0082	0.1476 \pm 0.0041/0.4530 \pm 0.0026	0.3987 \pm 0.0108/0.7558 \pm 0.0185	0.0339 \pm 0.0051/0.1111 \pm 0.0098
	M_f	0.6120 \pm 0.0013/0.9612 \pm 0.0021	0.2795 \pm 0.0014/0.8974 \pm 0.0042	0.7441 \pm 0.0060/0.7441 \pm 0.0060	0.2773 \pm 0.0215/0.9181 \pm 0.0102
Oversampling	M	0.2368 \pm 0.0197/0.3484 \pm 0.0041	0.0635 \pm 0.0184/0.4574 \pm 0.0496	0.3538 \pm 0.0063/0.7269 \pm 0.0346	0.0647 \pm 0.0165/0.2141 \pm 0.0710
	M_r	0.1452 \pm 0.0016/0.1452 \pm 0.0016	0.0447 \pm 0.0233/0.3330 \pm 0.0340	0.3341 \pm 0.0090/0.8059 \pm 0.0001	0.0392 \pm 0.0071/0.1818 \pm 0.0022
	M_f	0.2859 \pm 0.0176/0.2859 \pm 0.0249	0.1272 \pm 0.0001/0.6284 \pm 0.0720	0.6570 \pm 0.0623/0.6570 \pm 0.0623	0.0988 \pm 0.0477/0.2819 \pm 0.1707
Undersampling	M	0.2284 \pm 0.0126/0.3230 \pm 0.0391	0.0709 \pm 0.0226/0.4171 \pm 0.0357	0.3513 \pm 0.0069/0.7239 \pm 0.0102	0.0576 \pm 0.0121/0.3067 \pm 0.0292
	M_r	0.1422 \pm 0.0170/0.1422 \pm 0.0170	0.0544 \pm 0.0263/0.3017 \pm 0.0105	0.3328 \pm 0.0090/0.8143 \pm 0.0048	0.0382 \pm 0.0084/0.1742 \pm 0.0077
	M_f	0.2714 \pm 0.0143/0.7338 \pm 0.0898	0.1271 \pm 0.0174/0.5850 \pm 0.1189	0.6435 \pm 0.0144/0.6435 \pm 0.0144	0.0836 \pm 0.0353/0.5507 \pm 0.1273

Performance Comparison with Existing MTPP models Table 7 and Table 6 report time prediction performance and mark prediction performance, respectively, of *ours* and existing MTPP models

including FullyNN, THP, SAHP, AttNHP and Marked-LNM. Compared with existing MTPP models, *ours* demonstrates superior performance in both time prediction and mark prediction. For mark prediction, *ours* is the first MTPP model which addresses mark imbalance. For time prediction, the time for each mark m is predicted by drawing samples from $p^*(t|m)$ based on $\Gamma^*(m, t)$. The accurate approximation of $\Gamma^*(m, t)$ leads to accurate time prediction. In particular, *ours* also outperforms Marked-LNM in time prediction. This demonstrates that modeling $\Gamma^*(m, t)$ by neural networks is better than directly modeling $p^*(t|m)$ by the composition of log-normal distributions.

Table 7: Mark prediction performance to evaluate *ours* against existing MTPP models, measured by macro-F1/micro-F1. The bold are the best values.

		Retweet	SO	Taobao	USearhquake
ours	M	0.4750 \pm 0.0033/ 0.4394 \pm 0.0093	0.1776 \pm 0.0030/ 0.6376 \pm 0.0026	0.4190 \pm 0.0104/ 0.7499 \pm 0.0151	0.1382 \pm 0.0071/ 0.3189 \pm 0.0125
	M_r	0.2010 \pm 0.0082/ 0.2010 \pm 0.0082	0.1476 \pm 0.0041/ 0.4530 \pm 0.0026	0.3987 \pm 0.0108/ 0.7558 \pm 0.0185	0.0339 \pm 0.0051/ 0.1111 \pm 0.0098
	M_f	0.6120 \pm 0.0013/0.9612 \pm 0.0021	0.2795 \pm 0.0014/ 0.8974 \pm 0.0042	0.7441 \pm 0.0060/ 0.7441 \pm 0.0060	0.2773 \pm 0.0215/0.9181 \pm 0.0102
FullyNN	M	0.2190 \pm 0.0000/0.0000 \pm 0.0000	0.0054 \pm 0.0000/0.0000 \pm 0.0000	0.0094 \pm 0.0000/0.0000 \pm 0.0000	0.0914 \pm 0.0000/0.0000 \pm 0.0000
	M_r	0.0000 \pm 0.0000/0.0000 \pm 0.0000	0.0000 \pm 0.0000/0.0000 \pm 0.0000	0.0100 \pm 0.0000/0.7209 \pm 0.0000	0.0000 \pm 0.0000/0.0000 \pm 0.0000
	M_f	0.3284 \pm 0.0000/0.9768 \pm 0.0000	0.0236 \pm 0.0000/0.9155 \pm 0.0000	0.0000 \pm 0.0000/0.0000 \pm 0.0000	0.2134 \pm 0.0000/ 0.9457 \pm 0.0000
SAHP	M	0.4211 \pm 0.0050/0.1540 \pm 0.0480	0.1134 \pm 0.0027/0.5665 \pm 0.0059	0.0616 \pm 0.0327/0.1650 \pm 0.1574	0.0962 \pm 0.0005/0.1237 \pm 0.0060
	M_r	0.0266 \pm 0.0135/0.0266 \pm 0.0135	0.0863 \pm 0.0032/0.3500 \pm 0.0071	0.0269 \pm 0.0341/0.0825 \pm 0.1009	0.0037 \pm 0.0010/0.0162 \pm 0.0015
	M_f	0.6183 \pm 0.0010/0.9769 \pm 0.0001	0.2054 \pm 0.0011/0.9170 \pm 0.0005	0.6166 \pm 0.0112/0.6166 \pm 0.0112	0.2196 \pm 0.0016/0.9451 \pm 0.0002
THP	M	0.2238 \pm 0.0068/0.0000 \pm 0.0000	0.0859 \pm 0.0204/0.3984 \pm 0.1867	0.0069 \pm 0.0035/0.0000 \pm 0.0000	0.0921 \pm 0.0003/0.0000 \pm 0.0000
	M_r	0.0000 \pm 0.0000/0.0000 \pm 0.0000	0.0519 \pm 0.0270/0.2120 \pm 0.1360	0.0074 \pm 0.0037/0.7208 \pm 0.0001	0.0000 \pm 0.0000/0.0004 \pm 0.0006
	M_f	0.3357 \pm 0.0102/0.9768 \pm 0.0000	0.2015 \pm 0.0025/0.9140 \pm 0.0012	0.0000 \pm 0.0000/0.0000 \pm 0.0000	0.2149 \pm 0.0008/ 0.9457 \pm 0.0008
AttNHP	M	0.4100 \pm 0.0049/0.1901 \pm 0.0143	0.0594 \pm 0.0037/0.4548 \pm 0.0148	0.2930 \pm 0.0353/0.6359 \pm 0.0415	0.1306 \pm 0.0041/0.0809 \pm 0.0460
	M_r	0.0373 \pm 0.0056/0.0373 \pm 0.0056	0.0188 \pm 0.0000/0.2476 \pm 0.0029	0.2682 \pm 0.0363/0.5868 \pm 0.0604	0.0012 \pm 0.0007/0.0092 \pm 0.0079
	M_f	0.5963 \pm 0.0046/0.9747 \pm 0.0007	0.1972 \pm 0.0164/0.8372 \pm 0.0643	0.6901 \pm 0.0189/0.6901 \pm 0.0189	0.3031 \pm 0.0086/0.9434 \pm 0.0012
Marked-LNM	M	0.4216 \pm 0.0021/0.1565 \pm 0.0129	0.1323 \pm 0.0009/0.5995 \pm 0.0038	0.0911 \pm 0.0551/0.6658 \pm 0.0615	0.1056 \pm 0.0048/0.1130 \pm 0.0027
	M_r	0.0252 \pm 0.0041/0.0252 \pm 0.0041	0.1119 \pm 0.0001/0.3940 \pm 0.0055	0.0547 \pm 0.0577/0.6278 \pm 0.0884	0.0063 \pm 0.0072/0.0135 \pm 0.0006
	M_f	0.6198 \pm 0.0010/ 0.9769 \pm 0.0000	0.2016 \pm 0.0004/0.9123 \pm 0.0011	0.7077 \pm 0.0308/0.7077 \pm 0.0308	0.2380 \pm 0.0030/0.9451 \pm 0.0001

5 Related Work

Marked Temporal Point Process Many MTPP studies specify a separate Conditional Intensity Function (CIF) $\lambda^*(m, t)$ for each categorical mark m , based on which $p^*(m, t)$ can be formulated [10, 24, 44, 41, 12, 26, 29]. A more sophisticated intensity function [24, 44, 41, 26] can better capture the system dynamics but will require approximating the integral of $\lambda^*(m, t)$ using a numerical method such as Monte Carlo. Recurrent Marked Temporal Point Process(RMTPP) [11] eludes numerical integral approximation as the CIF and its integral have a closed form, which makes the log-likelihood easy to compute. Recent studies move away from directly modeling CIF. Shchur et al. [33] proposed an intensity-free solution, called LogNormMix, to infer the density function $p^*(t)$ from a simple distribution such as the mixture of log-normal distributions. Omi et al. [28] proposed FullyNN to model the integral of CIF using a neural network where CIF can be derived by differentiation, an operation computationally much easier compared with integration. All MTPP studies discussed so far predict the time of the next event first and then predict the mark. Recently, Waghmare et al. [36] proposes to model $p^*(m)$ using a classifier to predict the mark of the next event and modeling $p^*(t|m)$ to predict the time of the event based on LogNormMix.

Table 6: Time prediction performance to evaluate *ours* vs. existing MTPP models. The bold are the best values.

		Retweet	SO	Taobao	USearhquake
ours	M	2515.1 \pm 6.5029	0.5212 \pm 0.0142	0.3324 \pm 0.0579	0.6856 \pm 0.0063
	M_r	3291.2 \pm 29.097	0.4986 \pm 0.0175	0.3385 \pm 0.0627	0.6966 \pm 0.0081
	M_f	2198.7 \pm 2.4798	0.6063 \pm 0.0001	0.2529 \pm 0.0055	0.6713 \pm 0.0048
FullyNN	M	5126.0 \pm 854.88	0.7047 \pm 0.0203	6.5079 \pm 2.0854	1.2684 \pm 0.3715
	M_r	7525.4 \pm 1037.4	0.7231 \pm 0.0269	6.6713 \pm 2.1557	1.2709 \pm 0.3356
	M_f	4232.0 \pm 69.50	0.6461 \pm 0.0029	4.4131 \pm 1.3632	1.2671 \pm 0.4082
SAHP	M	3320.0 \pm 242.70	0.8010 \pm 0.0593	23.409 \pm 14.564	0.7608 \pm 0.0588
	M_r	4260.9 \pm 618.21	0.7882 \pm 0.0734	27.638 \pm 17.438	0.7777 \pm 0.0650
	M_f	2936.3 \pm 118.11	0.8493 \pm 0.0208	1.7466 \pm 0.8728	0.7388 \pm 0.0512
THP	M	3601.1 \pm 231.52	0.6433 \pm 0.0059	3.0100 \pm 2.2806	0.7322 \pm 0.0078
	M_r	4250.6 \pm 211.71	0.6586 \pm 0.0080	3.0036 \pm 2.2893	0.7409 \pm 0.0057
	M_f	3315.2 \pm 241.35	0.6097 \pm 0.0010	3.3648 \pm 1.0252	0.7207 \pm 0.0114
AttNHP	M	3551.1 \pm 12.611	7.9305 \pm 5.9188	5.4038 \pm 1.3280	6.4583 \pm 2.2939
	M_r	4406.5 \pm 7.518	6.8682 \pm 4.8605	5.2849 \pm 1.2944	6.6158 \pm 2.3176
	M_f	3187.8 \pm 10.646	13.197 \pm 11.171	7.7158 \pm 1.9980	6.2544 \pm 2.2619
Marked-LNM	M	2559.8 \pm 5.9380	0.9067 \pm 0.3687	0.2058 \pm 0.0079	0.7646 \pm 0.0026
	M_r	3314.3 \pm 1.2460	1.0520 \pm 0.5330	0.2043 \pm 0.0091	0.7773 \pm 0.0057
	M_f	2249.7 \pm 7.4050	0.6084 \pm 0.0007	0.2318 \pm 0.0128	0.7480 \pm 0.0013

Recently, Yuan et al. [40] use a Denoising Diffusion Probabilistic Model (DDPM) to predict the next event in the spatio-temporal point process. Lüdke et al. [23] develop Add-and-thin, a method for modifying event sequences sampled from a Poisson process to match a target distribution by adding or removing events. However, the mark of the spatio-temporal point process is continuous instead of discrete, and Add-and-thin is a temporal point process (TPP) model that does not consider mark. Therefore, these two approaches are out of the scope of our research.

Imbalanced Data Handling The techniques for handling imbalanced data, including data-level, algorithm-level, and classifier-level approaches, are designed mainly for improving imbalanced classification tasks. The data-level approach is resampling the training set, including undersampling and oversampling [3]. Most existing resampling methods are based on the Synthetic Minority Over-sampling Technique (SMOTE) algorithm [13, 6, 5]. One benefit of data-level approaches is that they can cooperate with any classifiers. In contrast, algorithm-level approaches are more classifier-specific, such as cost-sensitive methods [18, 21, 9]. The classifier-level method is also known as *thresholding* (or *post-scaling*) which learns thresholds to tune the obtained class probability [19, 7, 8, 35]. The effectiveness of resampling the train set is determined by the resampling ratio, but there is no easy way to figure it out for different classes on different datasets; The cost-sensitive approaches require domain knowledge regarding the importance of different marks to set the cost, but not always available [17]. To have a solution with minimum external knowledge and assumptions, this study adopts thresholding.

6 Conclusion and Limitation

Conclusion It is challenging for existing MTPP methods to accurately predict events of rare marks when the distribution of event marks is highly imbalanced. This is unacceptable in many applications if the rare mark is critical such as major earthquakes. This study introduces the first solution to address mark imbalance in MTPP. Instead of predicting mark based on mark probability directly as in existing studies, we learn thresholds to tune the mark probability normalized by the prior probability to optimize mark prediction. To achieve this goal, this study develops a strategy to predict mark first and then the time by integrating two improper integrations into one and proposing a novel Integration-free Neural Marked Temporal Point Process (IFNMTPP) to approximate the unified improper integration to support time sampling and estimation of mark probability, rather than using computationally expensive numerical improper integration. Extensive experiments on real-world datasets demonstrate the superior performance of our solution against various baselines in the next event mark and time prediction.

Limitation As the first effort to address the mark imbalance for MTPP, this study verifies the effectiveness of thresholding, but does not investigate (i) the opportunity to extend the thresholding method to incorporate domain knowledge, such as the importance of rare marks, and (ii) the effectiveness of resampling and cost-sensitive approaches in this situation.

Broader Impact

This paper presents work whose goal is to advance the field of Machine Learning. Specifically, we want to reveal the mark imbalance to the MTPP community and propose a relatively simple solution to inspire the development of more bias-aware MTPP approaches. There are many potential societal consequences of our work, none of which we feel must be specifically highlighted here.

Acknowledgement

This research is supported in part by the Australian Research Council (ARC) Discovery Projects DP200101441 and DP210100743.

References

- [1] G. Aguiar, B. Krawczyk, and A. Cano. A survey on learning from imbalanced data streams: Taxonomy, challenges, empirical study, and reproducible experimental framework. *Machine Learning*, 113(7):4165–4243, July 2024. ISSN 0885-6125, 1573-0565. doi: 10.1007/s10994-023-06353-6.
- [2] Alibaba. User behavior data from taobao for recommendation, 2018.
- [3] E. Aminian, R. P. Ribeiro, and J. Gama. Chebyshev approaches for imbalanced data streams regression models. *Data Mining and Knowledge Discovery*, 35(6):2389–2466, Nov. 2021. ISSN 1384-5810, 1573-756X. doi: 10.1007/s10618-021-00793-1.
- [4] M. Arastuie, S. Paul, and K. Xu. CHIP: A Hawkes Process Model for Continuous-time Networks with Scalable and Consistent Estimation. In *Advances in Neural Information Processing Systems*, volume 33, pages 16983–16996, 2020.
- [5] A. Bernardo and E. Della Valle. VFC-SMOTE: Very fast continuous synthetic minority oversampling for evolving data streams. *Data Mining and Knowledge Discovery*, 35(6):2679–2713, Nov. 2021. ISSN 1384-5810, 1573-756X. doi: 10.1007/s10618-021-00786-0.
- [6] A. Bernardo, H. M. Gomes, J. Montiel, B. Pfahringer, A. Bifet, and E. D. Valle. C-SMOTE: Continuous Synthetic Minority Oversampling for Evolving Data Streams. In *2020 IEEE International Conference on Big Data (Big Data)*, pages 483–492, Atlanta, GA, USA, Dec. 2020. IEEE. ISBN 978-1-7281-6251-5. doi: 10.1109/BigData50022.2020.9377768.
- [7] M. Buda, A. Maki, and M. A. Mazurowski. A systematic study of the class imbalance problem in convolutional neural networks. *Neural Networks*, 106:249–259, Oct. 2018. ISSN 08936080. doi: 10.1016/j.neunet.2018.07.011.
- [8] R. Chan, M. Rottmann, F. Hüger, P. Schlicht, and H. Gottschalk. Application of Decision Rules for Handling Class Imbalance in Semantic Segmentation, Jan. 2019.
- [9] Y. Chen, X. Yang, and H.-L. Dai. Cost-sensitive continuous ensemble kernel learning for imbalanced data streams with concept drift. *Knowledge-Based Systems*, 284:111272, Jan. 2024. ISSN 0950-7051. doi: 10.1016/j.knosys.2023.111272.
- [10] D. J. Daley. *An Introduction to the Theory of Point Processes: Volume I: Elementary Theory and Methods*. Probability and Its Applications Ser. Springer New York, New York, NY, 2nd ed edition, 2003. ISBN 978-0-387-21564-8.
- [11] N. Du, H. Dai, R. Trivedi, U. Upadhyay, M. Gomez-Rodriguez, and L. Song. Recurrent Marked Temporal Point Processes: Embedding Event History to Vector. In *Proceedings of the 22nd ACM SIGKDD International Conference on Knowledge Discovery and Data Mining*, pages 1555–1564, San Francisco California USA, Aug. 2016. ACM. ISBN 978-1-4503-4232-2. doi: 10.1145/2939672.2939875.
- [12] J. Enguehard, D. Busbridge, A. Bozson, C. Woodcock, and N. Hammerla. Neural Temporal Point Processes For Modelling Electronic Health Records. In *Proceedings of the Machine Learning for Health NeurIPS Workshop*, pages 85–113. PMLR, Nov. 2020.
- [13] A. Fernandez, S. Garcia, F. Herrera, and N. V. Chawla. SMOTE for Learning from Imbalanced Data: Progress and Challenges, Marking the 15-year Anniversary. *Journal of Artificial Intelligence Research*, 61:863–905, Apr. 2018. ISSN 1076-9757. doi: 10.1613/jair.1.11192.
- [14] A. G. Hawkes. Spectra of some self-exciting and mutually exciting point processes. *Biometrika*, 58(1):83–90, 1971. ISSN 0006-3444, 1464-3510. doi: 10.1093/biomet/58.1.83.
- [15] Z. Huang, H. Soliman, S. Paul, and K. S. Xu. A mutually exciting latent space Hawkes process model for continuous-time networks. In J. Cussens and K. Zhang, editors, *Uncertainty in Artificial Intelligence, Proceedings of the Thirty-Eighth Conference on Uncertainty in Artificial Intelligence*, UAI 2022, 1-5 August 2022, Eindhoven, The Netherlands, volume 180 of *Proceedings of Machine Learning Research*, pages 863–873. PMLR, 2022. doi: 10.48550/arXiv.2205.09263.

[16] T. Idé, G. Kollias, D. T. Phan, and N. Abe. Cardinality-Regularized Hawkes-Granger Model. In *Advances in Neural Information Processing Systems*, 2022. doi: 10.48550/arXiv.2208.10671.

[17] J. M. Johnson and T. M. Khoshgoftaar. Survey on deep learning with class imbalance. *Journal of Big Data*, 6(1):27, Dec. 2019. ISSN 2196-1115. doi: 10.1186/s40537-019-0192-5.

[18] B. Krawczyk and P. Skryjomska. Cost-sensitive perceptron decision trees for imbalanced drifting data streams. In M. Ceci, J. Hollmén, L. Todorovski, C. Vens, and S. Džeroski, editors, *Machine Learning and Knowledge Discovery in Databases*, pages 512–527, Cham, 2017. Springer International Publishing. ISBN 978-3-319-71246-8.

[19] S. Lawrence, I. Burns, A. Back, A. C. Tsoi, and C. L. Giles. Neural Network Classification and Prior Class Probabilities. In G. Montavon, G. B. Orr, and K.-R. Müller, editors, *Neural Networks: Tricks of the Trade*, volume 7700, pages 295–309. Springer Berlin Heidelberg, Berlin, Heidelberg, 2012. ISBN 978-3-642-35288-1 978-3-642-35289-8. doi: 10.1007/978-3-642-35289-8_19.

[20] J. Leskovec and A. Krevl. SNAP Datasets: Stanford large network dataset collection. <http://snap.stanford.edu/data>, June 2014.

[21] L. Loezer, F. Enembreck, J. P. Barddal, and A. de Souza Britto Jr. Cost-sensitive learning for imbalanced data streams. In *Proceedings of the 35th annual ACM symposium on applied computing*, pages 498–504, 2020.

[22] V. López, A. Fernández, J. G. Moreno-Torres, and F. Herrera. Analysis of preprocessing vs. cost-sensitive learning for imbalanced classification. Open problems on intrinsic data characteristics. *Expert Systems with Applications*, 39(7):6585–6608, June 2012. ISSN 09574174. doi: 10.1016/j.eswa.2011.12.043.

[23] D. Lüdke, M. Biloš, O. Shchur, M. Lienen, and S. Günnemann. Add and Thin: Diffusion for Temporal Point Processes. *Neural Information Processing Systems*, abs/2311.1139, 2023. doi: 10.48550/arXiv.2311.01139.

[24] H. Mei and J. Eisner. The Neural Hawkes Process: A Neurally Self-Modulating Multivariate Point Process. In I. Guyon, U. von Luxburg, S. Bengio, H. M. Wallach, R. Fergus, S. V. N. Vishwanathan, and R. Garnett, editors, *Advances in Neural Information Processing Systems 30: Annual Conference on Neural Information Processing Systems 2017, December 4-9, 2017, Long Beach, CA, USA*, pages 6754–6764, 2017.

[25] H. Mei, T. Wan, and J. Eisner. Noise-Contrastive Estimation for Multivariate Point Processes. In H. Larochelle, M. Ranzato, R. Hadsell, M. F. Balcan, and H. Lin, editors, *Advances in Neural Information Processing Systems*, volume 33, pages 5204–5214. Curran Associates, Inc., 2020.

[26] H. Mei, C. Yang, and J. Eisner. Transformer Embeddings of Irregularly Spaced Events and Their Participants. In *International Conference on Learning Representations*, Sept. 2021.

[27] M. Okawa, T. Iwata, Y. Tanaka, H. Toda, T. Kurashima, and H. Kashima. Dynamic Hawkes Processes for Discovering Time-evolving Communities’ States behind Diffusion Processes. In *KDD ’21: The 27th ACM SIGKDD Conference on Knowledge Discovery and Data Mining, KDD ’21*, pages 1276–1286, Virtual Event Singapore, Aug. 2021. ACM. ISBN 978-1-4503-8332-5. doi: 10.1145/3447548.3467248.

[28] T. Omi, N. Ueda, and K. Aihara. Fully Neural Network based Model for General Temporal Point Processes. In H. M. Wallach, H. Larochelle, A. Beygelzimer, F. d’Alché-Buc, E. B. Fox, and R. Garnett, editors, *Advances in Neural Information Processing Systems 32: Annual Conference on Neural Information Processing Systems 2019, NeurIPS 2019, December 8-14, 2019, Vancouver, BC, Canada*, pages 2120–2129, 2019.

[29] A. Panos. Decomposable Transformer Point Processes. *Neural Information Processing Systems*, abs/2409.18158, 2024. doi: 10.48550/arXiv.2409.18158.

[30] A. Paszke, S. Gross, F. Massa, A. Lerer, J. Bradbury, G. Chanan, T. Killeen, Z. Lin, N. Gimelshein, L. Antiga, A. Desmaison, A. Kopf, E. Yang, Z. DeVito, M. Raison, A. Tejani, S. Chilamkurthy, B. Steiner, L. Fang, J. Bai, and S. Chintala. PyTorch: An Imperative Style, High-Performance Deep Learning Library. In *Advances in Neural Information Processing Systems*, volume 32. Curran Associates, Inc., 2019.

[31] J. G. Rasmussen. Lecture Notes: Temporal Point Processes and the Conditional Intensity Function. [arXiv:1806.00221](https://arxiv.org/abs/1806.00221), 2018.

[32] M.-A. Rizoiu, L. Xie, S. Sanner, M. Cebrian, H. Yu, and P. Van Hentenryck. Expecting to be HIP: Hawkes Intensity Processes for Social Media Popularity. In *Proceedings of the 26th International Conference on World Wide Web, WWW '17*, pages 735–744, Perth Australia, Apr. 2017. International World Wide Web Conferences Steering Committee. ISBN 978-1-4503-4913-0. doi: 10.1145/3038912.3052650.

[33] O. Shchur, M. Bilos, and S. Günnemann. Intensity-Free Learning of Temporal Point Processes. In *8th International Conference on Learning Representations, ICLR 2020, Addis Ababa, Ethiopia, April 26-30, 2020*. OpenReview.net, 2020.

[34] O. Shchur, A. C. Türkmen, T. Januschowski, and S. Günnemann. Neural Temporal Point Processes: A Review. In *Proceedings of the Thirtieth International Joint Conference on Artificial Intelligence, IJCAI 2021, Virtual Event / Montreal, Canada, 19-27 August 2021*, pages 4585–4593, Montreal, Canada, Aug. 2021. International Joint Conferences on Artificial Intelligence Organization. ISBN 978-0-9992411-9-6. doi: 10.24963/ijcai.2021/623.

[35] J. Tian, Y.-C. Liu, N. Glaser, Y.-C. Hsu, and Z. Kira. Posterior Re-calibration for Imbalanced Datasets. In *Advances in Neural Information Processing Systems*, volume 33, pages 8101–8113. Curran Associates, Inc., 2020.

[36] G. Waghmare, A. Debnath, S. Asthana, and A. Malhotra. Modeling Inter-Dependence Between Time and Mark in Multivariate Temporal Point Processes. In *CIKM '22: The 31st ACM International Conference on Information and Knowledge Management*, pages 1986–1995, Atlanta GA USA, Oct. 2022. ACM. ISBN 978-1-4503-9236-5. doi: 10.1145/3511808.3557399.

[37] T. Xiao, Z. Xu, W. He, Z. Xiao, Y. Zhang, Z. Liu, S. Chen, M. T. Thai, J. Bian, P. Rashidi, and Z. Jiang. XTSFormer: Cross-Temporal-Scale Transformer for Irregular-Time Event Prediction in Clinical Applications. *AAAI Conference on Artificial Intelligence*, 39:28502–28510, Apr. 2025. doi: 10.1609/aaai.v39i27.35073.

[38] S. Xue, X. Shi, Z. Chu, Y. Wang, F. Zhou, H. Hao, C. Jiang, C. Pan, Y. Xu, J. Y. Zhang, Q. Wen, J. Zhou, and H. Mei. EasyTPP: Towards Open Benchmarking Temporal Point Processes. *International Conference on Learning Representations*, 2023. doi: 10.48550/arXiv.2307.08097.

[39] L. Yang, H. Jiang, Q. Song, and J. Guo. A Survey on Long-Tailed Visual Recognition. *International Journal of Computer Vision*, 130(7):1837–1872, July 2022. ISSN 0920-5691, 1573-1405. doi: 10.1007/s11263-022-01622-8.

[40] Y. Yuan, J. Ding, C. Shao, D. Jin, and Y. Li. Spatio-temporal Diffusion Point Processes. In *Proceedings of the 29th ACM SIGKDD Conference on Knowledge Discovery and Data Mining, KDD '23*, pages 3173–3184, Long Beach CA USA, Aug. 2023. ACM. ISBN 979-8-4007-0103-0. doi: 10.1145/3580305.3599511.

[41] Q. Zhang, A. Lipani, O. Kirnap, and E. Yilmaz. Self-Attentive Hawkes Process. In *Proceedings of the 37th International Conference on Machine Learning*, pages 11183–11193. PMLR, Nov. 2020.

[42] Q. Zhao, M. A. Erdogdu, H. Y. He, A. Rajaraman, and J. Leskovec. SEISMIC: A Self-Exciting Point Process Model for Predicting Tweet Popularity. In *Proceedings of the 21th ACM SIGKDD International Conference on Knowledge Discovery and Data Mining, Sydney, NSW, Australia, August 10-13, 2015*, pages 1513–1522, Sydney NSW Australia, Aug. 2015. ACM. ISBN 978-1-4503-3664-2. doi: 10.1145/2783258.2783401.

- [43] Z. Zhou and R. Yu. Automatic Integration for Spatiotemporal Neural Point Processes. Neural Information Processing Systems, abs/2310.6179, 2023. doi: 10.48550/arXiv.2310.06179.
- [44] S. Zuo, H. Jiang, Z. Li, T. Zhao, and H. Zha. Transformer Hawkes Process. In Proceedings of the 37th International Conference on Machine Learning, pages 11692–11702. PMLR, Nov. 2020.

NeurIPS Paper Checklist

1. Claims

Question: Do the main claims made in the abstract and introduction accurately reflect the paper's contributions and scope?

Answer: [\[Yes\]](#)

Justification: The contribution of this paper is first realizing the impact of mark imbalance to event predictions of MTPPs then devising an MTPP model and additional techniques to tackle this issue. They are reflected in our abstract and introduction.

Guidelines:

- The answer NA means that the abstract and introduction do not include the claims made in the paper.
- The abstract and/or introduction should clearly state the claims made, including the contributions made in the paper and important assumptions and limitations. A No or NA answer to this question will not be perceived well by the reviewers.
- The claims made should match theoretical and experimental results, and reflect how much the results can be expected to generalize to other settings.
- It is fine to include aspirational goals as motivation as long as it is clear that these goals are not attained by the paper.

2. Limitations

Question: Does the paper discuss the limitations of the work performed by the authors?

Answer: [\[Yes\]](#)

Justification: We have discussed the limit of our work in the main paper.

Guidelines:

- The answer NA means that the paper has no limitation while the answer No means that the paper has limitations, but those are not discussed in the paper.
- The authors are encouraged to create a separate "Limitations" section in their paper.
- The paper should point out any strong assumptions and how robust the results are to violations of these assumptions (e.g., independence assumptions, noiseless settings, model well-specification, asymptotic approximations only holding locally). The authors should reflect on how these assumptions might be violated in practice and what the implications would be.
- The authors should reflect on the scope of the claims made, e.g., if the approach was only tested on a few datasets or with a few runs. In general, empirical results often depend on implicit assumptions, which should be articulated.
- The authors should reflect on the factors that influence the performance of the approach. For example, a facial recognition algorithm may perform poorly when image resolution is low or images are taken in low lighting. Or a speech-to-text system might not be used reliably to provide closed captions for online lectures because it fails to handle technical jargon.
- The authors should discuss the computational efficiency of the proposed algorithms and how they scale with dataset size.
- If applicable, the authors should discuss possible limitations of their approach to address problems of privacy and fairness.
- While the authors might fear that complete honesty about limitations might be used by reviewers as grounds for rejection, a worse outcome might be that reviewers discover limitations that aren't acknowledged in the paper. The authors should use their best judgment and recognize that individual actions in favor of transparency play an important role in developing norms that preserve the integrity of the community. Reviewers will be specifically instructed to not penalize honesty concerning limitations.

3. Theory assumptions and proofs

Question: For each theoretical result, does the paper provide the full set of assumptions and a complete (and correct) proof?

Answer: [\[Yes\]](#)

Justification: We provide the complete proof of how to obtain $p^*(m, t)$ in Appendix A and $\Gamma^*(m, t)$ in the main paper.

Guidelines:

- The answer NA means that the paper does not include theoretical results.
- All the theorems, formulas, and proofs in the paper should be numbered and cross-referenced.
- All assumptions should be clearly stated or referenced in the statement of any theorems.
- The proofs can either appear in the main paper or the supplemental material, but if they appear in the supplemental material, the authors are encouraged to provide a short proof sketch to provide intuition.
- Inversely, any informal proof provided in the core of the paper should be complemented by formal proofs provided in appendix or supplemental material.
- Theorems and Lemmas that the proof relies upon should be properly referenced.

4. Experimental result reproducibility

Question: Does the paper fully disclose all the information needed to reproduce the main experimental results of the paper to the extent that it affects the main claims and/or conclusions of the paper (regardless of whether the code and data are provided or not)?

Answer: [\[Yes\]](#)

Justification: We have provided information including datasets, hyperparameters, technical details for reproducibility.

Guidelines:

- The answer NA means that the paper does not include experiments.
- If the paper includes experiments, a No answer to this question will not be perceived well by the reviewers: Making the paper reproducible is important, regardless of whether the code and data are provided or not.
- If the contribution is a dataset and/or model, the authors should describe the steps taken to make their results reproducible or verifiable.
- Depending on the contribution, reproducibility can be accomplished in various ways. For example, if the contribution is a novel architecture, describing the architecture fully might suffice, or if the contribution is a specific model and empirical evaluation, it may be necessary to either make it possible for others to replicate the model with the same dataset, or provide access to the model. In general, releasing code and data is often one good way to accomplish this, but reproducibility can also be provided via detailed instructions for how to replicate the results, access to a hosted model (e.g., in the case of a large language model), releasing of a model checkpoint, or other means that are appropriate to the research performed.
- While NeurIPS does not require releasing code, the conference does require all submissions to provide some reasonable avenue for reproducibility, which may depend on the nature of the contribution. For example
 - (a) If the contribution is primarily a new algorithm, the paper should make it clear how to reproduce that algorithm.
 - (b) If the contribution is primarily a new model architecture, the paper should describe the architecture clearly and fully.
 - (c) If the contribution is a new model (e.g., a large language model), then there should either be a way to access this model for reproducing the results or a way to reproduce the model (e.g., with an open-source dataset or instructions for how to construct the dataset).
 - (d) We recognize that reproducibility may be tricky in some cases, in which case authors are welcome to describe the particular way they provide for reproducibility. In the case of closed-source models, it may be that access to the model is limited in some way (e.g., to registered users), but it should be possible for other researchers to have some path to reproducing or verifying the results.

5. Open access to data and code

Question: Does the paper provide open access to the data and code, with sufficient instructions to faithfully reproduce the main experimental results, as described in supplemental material?

Answer: [Yes]

Justification: A sample code with running scripts and instructions are available in our supplementary material. They will be publically available upon acceptance.

Guidelines:

- The answer NA means that paper does not include experiments requiring code.
- Please see the NeurIPS code and data submission guidelines (<https://nips.cc/public/guides/CodeSubmissionPolicy>) for more details.
- While we encourage the release of code and data, we understand that this might not be possible, so “No” is an acceptable answer. Papers cannot be rejected simply for not including code, unless this is central to the contribution (e.g., for a new open-source benchmark).
- The instructions should contain the exact command and environment needed to run to reproduce the results. See the NeurIPS code and data submission guidelines (<https://nips.cc/public/guides/CodeSubmissionPolicy>) for more details.
- The authors should provide instructions on data access and preparation, including how to access the raw data, preprocessed data, intermediate data, and generated data, etc.
- The authors should provide scripts to reproduce all experimental results for the new proposed method and baselines. If only a subset of experiments are reproducible, they should state which ones are omitted from the script and why.
- At submission time, to preserve anonymity, the authors should release anonymized versions (if applicable).
- Providing as much information as possible in supplemental material (appended to the paper) is recommended, but including URLs to data and code is permitted.

6. Experimental setting/details

Question: Does the paper specify all the training and test details (e.g., data splits, hyper-parameters, how they were chosen, type of optimizer, etc.) necessary to understand the results?

Answer: [Yes]

Justification: All training details are covered in the Appendix.

Guidelines:

- The answer NA means that the paper does not include experiments.
- The experimental setting should be presented in the core of the paper to a level of detail that is necessary to appreciate the results and make sense of them.
- The full details can be provided either with the code, in appendix, or as supplemental material.

7. Experiment statistical significance

Question: Does the paper report error bars suitably and correctly defined or other appropriate information about the statistical significance of the experiments?

Answer: [Yes]

Justification: We report the 1-sigma error on all experiment results and state this fact at the beginning of the experiment section.

Guidelines:

- The answer NA means that the paper does not include experiments.
- The authors should answer “Yes” if the results are accompanied by error bars, confidence intervals, or statistical significance tests, at least for the experiments that support the main claims of the paper.
- The factors of variability that the error bars are capturing should be clearly stated (for example, train/test split, initialization, random drawing of some parameter, or overall run with given experimental conditions).

- The method for calculating the error bars should be explained (closed form formula, call to a library function, bootstrap, etc.)
- The assumptions made should be given (e.g., Normally distributed errors).
- It should be clear whether the error bar is the standard deviation or the standard error of the mean.
- It is OK to report 1-sigma error bars, but one should state it. The authors should preferably report a 2-sigma error bar than state that they have a 96% CI, if the hypothesis of Normality of errors is not verified.
- For asymmetric distributions, the authors should be careful not to show in tables or figures symmetric error bars that would yield results that are out of range (e.g. negative error rates).
- If error bars are reported in tables or plots, The authors should explain in the text how they were calculated and reference the corresponding figures or tables in the text.

8. Experiments compute resources

Question: For each experiment, does the paper provide sufficient information on the computer resources (type of compute workers, memory, time of execution) needed to reproduce the experiments?

Answer: **[Yes]**

Justification: We expressed that we use A100 GPUs to run our experiments in the Appendix.

Guidelines:

- The answer NA means that the paper does not include experiments.
- The paper should indicate the type of compute workers CPU or GPU, internal cluster, or cloud provider, including relevant memory and storage.
- The paper should provide the amount of compute required for each of the individual experimental runs as well as estimate the total compute.
- The paper should disclose whether the full research project required more compute than the experiments reported in the paper (e.g., preliminary or failed experiments that didn't make it into the paper).

9. Code of ethics

Question: Does the research conducted in the paper conform, in every respect, with the NeurIPS Code of Ethics <https://neurips.cc/public/EthicsGuidelines>?

Answer: **[Yes]**

Justification: This work does not involve human subjects or participants. The datasets are publically available without copyright requirements. We also can not find any social harm, such as safety issues, security issues, discrimination, etc., that our approach may cause.

Guidelines:

- The answer NA means that the authors have not reviewed the NeurIPS Code of Ethics.
- If the authors answer No, they should explain the special circumstances that require a deviation from the Code of Ethics.
- The authors should make sure to preserve anonymity (e.g., if there is a special consideration due to laws or regulations in their jurisdiction).

10. Broader impacts

Question: Does the paper discuss both potential positive societal impacts and negative societal impacts of the work performed?

Answer: **[Yes]**

Justification: We have a broader impact discussing the potential impact of our approach at the end of the Appendix.

Guidelines:

- The answer NA means that there is no societal impact of the work performed.
- If the authors answer NA or No, they should explain why their work has no societal impact or why the paper does not address societal impact.

- Examples of negative societal impacts include potential malicious or unintended uses (e.g., disinformation, generating fake profiles, surveillance), fairness considerations (e.g., deployment of technologies that could make decisions that unfairly impact specific groups), privacy considerations, and security considerations.
- The conference expects that many papers will be foundational research and not tied to particular applications, let alone deployments. However, if there is a direct path to any negative applications, the authors should point it out. For example, it is legitimate to point out that an improvement in the quality of generative models could be used to generate deepfakes for disinformation. On the other hand, it is not needed to point out that a generic algorithm for optimizing neural networks could enable people to train models that generate Deepfakes faster.
- The authors should consider possible harms that could arise when the technology is being used as intended and functioning correctly, harms that could arise when the technology is being used as intended but gives incorrect results, and harms following from (intentional or unintentional) misuse of the technology.
- If there are negative societal impacts, the authors could also discuss possible mitigation strategies (e.g., gated release of models, providing defenses in addition to attacks, mechanisms for monitoring misuse, mechanisms to monitor how a system learns from feedback over time, improving the efficiency and accessibility of ML).

11. Safeguards

Question: Does the paper describe safeguards that have been put in place for responsible release of data or models that have a high risk for misuse (e.g., pretrained language models, image generators, or scraped datasets)?

Answer: [NA]

Justification: Our paper poses no such risks of misuse.

Guidelines:

- The answer NA means that the paper poses no such risks.
- Released models that have a high risk for misuse or dual-use should be released with necessary safeguards to allow for controlled use of the model, for example by requiring that users adhere to usage guidelines or restrictions to access the model or implementing safety filters.
- Datasets that have been scraped from the Internet could pose safety risks. The authors should describe how they avoided releasing unsafe images.
- We recognize that providing effective safeguards is challenging, and many papers do not require this, but we encourage authors to take this into account and make a best faith effort.

12. Licenses for existing assets

Question: Are the creators or original owners of assets (e.g., code, data, models), used in the paper, properly credited and are the license and terms of use explicitly mentioned and properly respected?

Answer: [Yes]

Justification: We have presented the creators and owners of all assets we used in our paper.

Guidelines:

- The answer NA means that the paper does not use existing assets.
- The authors should cite the original paper that produced the code package or dataset.
- The authors should state which version of the asset is used and, if possible, include a URL.
- The name of the license (e.g., CC-BY 4.0) should be included for each asset.
- For scraped data from a particular source (e.g., website), the copyright and terms of service of that source should be provided.
- If assets are released, the license, copyright information, and terms of use in the package should be provided. For popular datasets, paperswithcode.com/datasets has curated licenses for some datasets. Their licensing guide can help determine the license of a dataset.

- For existing datasets that are re-packaged, both the original license and the license of the derived asset (if it has changed) should be provided.
- If this information is not available online, the authors are encouraged to reach out to the asset's creators.

13. New assets

Question: Are new assets introduced in the paper well documented and is the documentation provided alongside the assets?

Answer: [Yes]

Justification: These documents are available alongside the code.

Guidelines:

- The answer NA means that the paper does not release new assets.
- Researchers should communicate the details of the dataset/code/model as part of their submissions via structured templates. This includes details about training, license, limitations, etc.
- The paper should discuss whether and how consent was obtained from people whose asset is used.
- At submission time, remember to anonymize your assets (if applicable). You can either create an anonymized URL or include an anonymized zip file.

14. Crowdsourcing and research with human subjects

Question: For crowdsourcing experiments and research with human subjects, does the paper include the full text of instructions given to participants and screenshots, if applicable, as well as details about compensation (if any)?

Answer: [NA]

Justification: This paper does not involve crowdsourcing nor research with human subjects.

Guidelines:

- The answer NA means that the paper does not involve crowdsourcing nor research with human subjects.
- Including this information in the supplemental material is fine, but if the main contribution of the paper involves human subjects, then as much detail as possible should be included in the main paper.
- According to the NeurIPS Code of Ethics, workers involved in data collection, curation, or other labor should be paid at least the minimum wage in the country of the data collector.

15. Institutional review board (IRB) approvals or equivalent for research with human subjects

Question: Does the paper describe potential risks incurred by study participants, whether such risks were disclosed to the subjects, and whether Institutional Review Board (IRB) approvals (or an equivalent approval/review based on the requirements of your country or institution) were obtained?

Answer: [NA]

Justification: This paper does not involve crowdsourcing nor research with human subjects.

Guidelines:

- The answer NA means that the paper does not involve crowdsourcing nor research with human subjects.
- Depending on the country in which research is conducted, IRB approval (or equivalent) may be required for any human subjects research. If you obtained IRB approval, you should clearly state this in the paper.
- We recognize that the procedures for this may vary significantly between institutions and locations, and we expect authors to adhere to the NeurIPS Code of Ethics and the guidelines for their institution.
- For initial submissions, do not include any information that would break anonymity (if applicable), such as the institution conducting the review.

16. Declaration of LLM usage

Question: Does the paper describe the usage of LLMs if it is an important, original, or non-standard component of the core methods in this research? Note that if the LLM is used only for writing, editing, or formatting purposes and does not impact the core methodology, scientific rigorousness, or originality of the research, declaration is not required.

Answer: [NA]

Justification: The LLM is used only for writing, editing, or formatting purposes and does not impact the core methodology, scientific rigorousness, or originality of the research.

Guidelines:

- The answer NA means that the core method development in this research does not involve LLMs as any important, original, or non-standard components.
- Please refer to our LLM policy (<https://neurips.cc/Conferences/2025/LLM>) for what should or should not be described.

A The Conditional Joint PDF

This study concerns events with categorical marks. For mark m , we define a conditional intensity function $\lambda^*(m, t)$:

$$\begin{aligned}
\lambda^*(m = k_i, t) &= \lambda(m = k_i, t | \mathcal{H}_t) \\
&= \lim_{\Delta t \rightarrow 0} \frac{P(m = k_i, t \in [t, t + \Delta t) | \mathcal{H}_{t-})}{\Delta t} \\
&= \lim_{\Delta t \rightarrow 0} \frac{p(m = k_i, t \in [t, t + \Delta t) | \mathcal{H}_{t_l}) \Delta t}{P(\forall j \in \mathbb{N}^+, t_j \notin (t_l, t) | \mathcal{H}_{t_l}) \Delta t} \\
&= \lim_{\Delta t \rightarrow 0} \frac{p(m = k_i, t \in [t, t + \Delta t) | \mathcal{H}_{t_l})}{P(\forall j \in \mathbb{N}^+, t_j \notin (t_l, t) | \mathcal{H}_{t_l})} \\
&= \frac{p(m = k_i, t \in [t, t + dt) | \mathcal{H}_{t_l})}{P(\forall j \in \mathbb{N}^+, t_j \notin (t_l, t) | \mathcal{H}_{t_l})}
\end{aligned} \tag{17}$$

where \mathcal{H}_{t_l} is the history up to (including) the most recent event, \mathcal{H}_{t-} is the history up to (excluding) the current time, $P(\forall j \in \mathbb{N}^+, t_j \notin (t_l, t) | \mathcal{H}_{t_l})$ represents the probability that no event is observed in time interval (t_l, t) given \mathcal{H}_{t_l} .

We denote $P'_m((t_1, t_2) | \mathcal{H}_{t_l})$ for the conditional probability that an event m happens in (t_1, t_2) . Following the definition of simple TPP that at most one event happens at every timestamp t , the probability that no event occurs in (t_l, t) is:

$$\begin{aligned}
&P(\forall j \in \mathbb{N}^+, t_j \notin (t_l, t) | \mathcal{H}_{t_l}) \\
&= 1 - \sum_{m \in M} P'_m((t_l, t) | \mathcal{H}_{t_l}) \prod_{n \in M, n \neq m} (1 - P'_n((t_l, t) | \mathcal{H}_{t_l})) \\
&= 1 - \sum_{m \in M} \frac{P'_m((t_l, t) | \mathcal{H}_{t_l})}{1 - P'_m((t_l, t) | \mathcal{H}_{t_l})} \prod_{n \in M} (1 - P'_n((t_l, t) | \mathcal{H}_{t_l})) \\
&= 1 - \sum_{m \in M} F(m, t | \mathcal{H}_{t_l}) = 1 - \sum_{m \in M} F^*(m, t)
\end{aligned} \tag{18}$$

where

$$F^*(m, t) = \frac{P'_m((t_l, t) | \mathcal{H}_{t_l})}{1 - P'_m((t_l, t) | \mathcal{H}_{t_l})} \prod_{n \in M} (1 - P'_n((t_l, t) | \mathcal{H}_{t_l})) \tag{19}$$

The conditional joint PDF that the next event is m and occurs in $[t, t + dt)$ is:

$$p(m = k_i, t \in [t, t + \Delta t) | \mathcal{H}_{t_l}) = \frac{dF^*(m = k_i, t)}{dt} \tag{20a}$$

$$\int_{t_l}^t p(m = k_i, t \in [t, t + \Delta t) | \mathcal{H}_{t_l}) d\tau = F^*(m = k_i, t) \tag{20b}$$

In this study, $p^*(m, t)$, shorthand of $p(m, t | \mathcal{H}_{t_l})$, is the formal representation of $p(m = k_i, t \in [t, t + \Delta t) | \mathcal{H}_{t_l})$. Note $F^*(m, t)$ in Equation (19) is the probability that only one event happens in interval $[t, t + dt)$ and the mark is m . This ensures the MTPP represented by $p^*(m, t)$ is simple. By integrating Equation (20a) and Equation (18) in Equation (17), we have

$$p^*(m, t) = \lambda^*(m, t) (1 - \sum_{w \in M} F^*(w, t)) \tag{21}$$

where $\sum_{w \in M} F^*(w, t)$ is calculated from the sum of Equation (17) over marker m :

$$\sum_{w \in M} F^*(w, t) = 1 - \exp(- \int_{t_l}^t \sum_{n \in M} \lambda^*(n, \tau) d\tau) \tag{22}$$

Then, we solve $p^*(m, t)$:

$$p^*(m, t) = \lambda^*(m, t) \exp(- \int_{t_l}^t \sum_{n \in M} \lambda^*(n, \tau) d\tau) \tag{23}$$

which is equivalent with Equation (2).

B Proof of the Proposition 3.1

Proof. The gradient of IFNMTPP is $-p^*(m, t)$, the function it learns must take the form:

$$\text{IFNMTPP}(m, t) = - \int_{C_1}^t p^*(m, \tau) d\tau + C_2 \quad (24)$$

where C_1 and C_2 are two constants.

From IFNMTPP architecture, the Integral Estimation Module (IEM) consists of multiple fully connected layers with non-negative weights, and monotonic increasing and unbounded activation functions. Then, it ends with a monotonic decreasing function $\sigma(x) = \frac{1}{1+e^x}$ (as illustrated in Figure 2). Since $\lim_{x \rightarrow +\infty} \sigma(x) = 0$, we have:

$$\lim_{t \rightarrow +\infty} \text{IFNMTPP}(m, t) = \lim_{t \rightarrow +\infty} - \int_{C_1}^t p^*(m, \tau) d\tau + C_2 = 0 \quad (25)$$

Substituting this into the earlier equation, we obtain:

$$C_2 = \lim_{t \rightarrow +\infty} \int_{C_1}^t p^*(m, \tau) d\tau = \int_{C_1}^{+\infty} p^*(m, \tau) d\tau \quad (26)$$

Substituting C_2 back in Equation (24):

$$\text{IFNMTPP}(m, t) = \int_{C_1}^{+\infty} p^*(m, \tau) d\tau - \int_{C_1}^t p^*(m, \tau) d\tau = \int_t^{+\infty} p^*(m, \tau) d\tau = \Gamma^*(m, t) \quad (27)$$

Thus, the output of IFNMTPP is $\Gamma^*(m, t)$ when its gradient is $-p^*(m, t)$. \square

C Technical Details

C.1 Technical Details about IFNMTPP

In Section B, we show that IFNMTPP models $\Gamma^*(m, t)$ when the activation function in the Integral Estimation Module (IEM) is monotonic increasing and unbounded. However, we select `tanh` as the activation function for training stability in the implementation. `tanh` is monotonic but bounded, so $\lim_{x \rightarrow +\infty} \text{IFNMTPP}(m, t) = C > 0$, making the implemented IFNMTPP slightly inaccurate. To mitigate this issue, we subtract the original output from the implemented IFNMTPP with C . The pseudo code is below:

```

1  for layer_idx, layer in enumerate(self.mlp):
2      # Hidden status at t for calculating \Gamma^*(m, t)
3      output = layer(output)
4      output = self.layer_activation(output)
5
6      # Hidden status at t_1 for calculating \Gamma^*(m, t_1)
7      output_zero = layer(output_zero)
8      output_zero = self.layer_activation(output_zero)
9
10     if layer_idx == 0:
11         # Hidden status at infinity for calculating \Gamma^*(m, +\infty)
12         a.k.a. C.
13         output_max = torch.ones_like(output) * self.tanh_parameter
14     else:
15         output_max = layer(output_max)
16         output_max = self.layer_activation(output_max)
17
18     probability_integral_from_t_to_inf = self.nonneg_integral(-self.aggregate
19     (output))
20     probability_integral_from_t1_to_inf = self.nonneg_integral(-self.
21     aggregate(output_zero))

```

```

21 probability_integral_minimal = self.nonneg_integral(-self.aggregate(
22     output_max))
23
24 # Shift the output with C when required.
25 if self.removes_tail:
26     regularized_probability_integral_from_t_to_inf = (
27         probability_integral_from_t_to_inf - probability_integral_minimal)
28
29     regularized_probability_integral_from_t1_to_inf = (
30         probability_integral_from_t1_to_inf - probability_integral_minimal) +
31         self.epsilon
32
33 else:
34     regularized_probability_integral_from_t_to_inf =
35     probability_integral_from_t_to_inf
36
37     regularized_probability_integral_from_t1_to_inf =
38     probability_integral_from_t1_to_inf + self.epsilon

```

C.2 Technical Details about Thresholding

We use the classic threshold-tuning method [19, 7] to obtain the optimal ϵ_m . Specifically, the method obtains optimal ϵ_m by taking three steps for each mark m . In step 1, we draw the precision-recall curve of m . This curve shows us the precision and recall across all possible thresholds. In step 2, since our target is to maximize the F1 score, which is the harmonic mean of the precision and recall, we compute the F1 score for all possible threshold using the precision and recall obtained in the first step. In step 3, the threshold that yields the maximum F1 value is the ϵ_m . The pseudo code is below:

```

1 # For each mark $m \in M$:
2 for i in range(num_events):
3
4     # Step 1: draw the precision-recall curve.
5     precision[i], recall[i], thresholds = precision_recall_curve((
6         training_results_events_next == i).astype(int),
7         scaled_training_results_pm[:, i])
8
9     # Step 2: Calculate the F1 score across all possible threshold.
10    f1s = (2 * precision[i] * recall[i]) / (precision[i] + recall[i])
11    f1s = np.nan_to_num(f1s)
12
13    # Step 3: Pick the threshold that yields the maximal F1 value.
14    ix = np.argmax(f1s)
15    f1[i] = f1s[ix]
16    threshold.append(thresholds[ix])

```

Once ϵ_m is known for each mark $m \in M$, we predict the next mark as m if $r_m - \epsilon_m$ is maximum. Why? because such m will lead to a higher F1 value compared to other marks.

Please note that we did not train a machine learning model like a neural network to obtain the optimal ϵ_m . Conceptually, one can predict m by selecting m with the maximum $r_m - \epsilon_m$ (i.e., *argmax*) and use the prediction loss to update the parameters of the model producing ϵ_m . However, *argmax* is non-differentiable so that backpropagation is not allowed to update model parameters. This is why we did not use this method.

D Experiment Settings

D.1 Real-world Datasets

We use the following four datasets to evaluate the performance of IFNMTPP.

- *Retweet dataset*[42] records when users Retweet a particular message on Twitter. This dataset distinguishes all users into three different types: (1) normal user, whose followers

count is lower than the median, (2) influence user, whose followers count is higher than the median but lower than the 95th percentile, (3) famous user, whose followers count is higher than the 95th percentile. About 2 million Retweets are recorded, and the average sequence length is 108. This dataset is released under the Apache-2.0 license[38].

- *StackOverflow dataset(SO)*[20] was collected from Stackoverflow⁵, a popular question-answering website about various topics. Users providing decent answers will receive different badges as rewards. This dataset collects the timestamps when people obtain 22 badges from the website, and the average sequence length is 72. This dataset is released under the Apache-2.0 license[38].
- *Taobao*[2] records users' interactions on Taobao, an online shopping website from China. These actions include user clicking and buying online items, viewing reviews and comments, or searching for items. The average length of sequences in this dataset is 58, and 17 different marks are available. This dataset is released under the Apache-2.0 license[38].
- *USearthquake*[38] records all earthquakes happened in the continental US from USGS⁶. This dataset has 7 marks, referring to earthquakes with magnitude 2.0 to 2.9, 3.0 to 3.9, 4.0 to 4.9, 5.0 to 5.9, 6.0 to 6.9, 7.0 to 7.9, or 8 and higher. The average sequence length is 16. This dataset is released under the Apache-2.0 license[38].

D.2 Synthetic Datasets

All synthetic datasets are generated so we do not have any licenses information for them. The code to generate all synthetic datasets comes from the codebase of [28] at <https://github.com/omitakahiro/NeuralNetworkPointProcess> which is publicly accessible without any licenses.

- *Hawkes process dataset Hawkes_1* was generated utilising Hawkes process:

$$\lambda^*(t) = \mu_0 + \sum_{t_i < t} a \exp(-b(t - t_i)) \quad (28)$$

where $\mu = 0.2$, $a = 0.8$, and $b = 1.0$.

- *Hawkes process dataset Hawkes_2* was generated utilising Hawkes process:

$$\lambda^*(t) = \mu_0 + \sum_{t_i < t} a_1 \exp(-b_1(t - t_i)) + a_2 \exp(-b_2(t - t_i)) \quad (29)$$

where $\mu = 0.2$, $a_1 = a_2 = 0.4$, $b_1 = 1.0$, and $b_2 = 20$.

- *Homogeneous Poisson process dataset* was generated using the Homogeneous Poisson process where the conditional intensity function $\lambda^*(t)$ is constant over the entire timeline. This paper assumes $\lambda^*(t) = 1$.
- *Self-correct process dataset* was generated using the temporal point process whose intensity significantly drops when an event happens. The definition of the conditional intensity function is $\lambda^*(t) = \exp(\mu(t - t_i) - \alpha N)$ where N is the number of occurred events, and μ and α are fixed parameters. In our experiments, we set $\alpha = \mu = 1$.
- *Stationary renewal process dataset* was generated using stationary renewal process, which directly defines the probability distribution over time $p^*(t)$ as a log-normal distribution as shown in Equation (30).

$$p^*(t|\sigma) = \frac{1}{\sigma t \sqrt{2\pi}} \exp\left(-\frac{\log^2(t)}{2\sigma^2}\right) \quad (30)$$

where σ is the standard deviation. Here, we set $\sigma = 1$. With Equation (30) and TPP's definition, one could solve the corresponding intensity function by Wolframalpha⁷:

$$\lambda^*(t) = \frac{-0.797885 \exp(-0.5 \log^2(t))}{-t + t \operatorname{erf}(0.707107 \log(t))} \quad (31)$$

where $\operatorname{erf}(x) = \frac{2}{\sqrt{\pi}} \int_0^x \exp(-t^2) dt$.

⁵<https://StackOverflow.com/>

⁶<http://earthquake.usgs.gov/earthquakes/eqarchives/year/eqstats.php>

⁷<https://www.wolframalpha.com>

These five synthetic distributions cooperate with a synthetic marking methods. This method generates discrete marks sampled from a uniform distribution. All synthetic datasets have 5 different marks.

D.3 Metrics

D.3.1 Metrics for Synthetic Datasets

For synthetic datasets, the real distribution $\hat{p}^*(m, t)$ is known. We can compare the generated $p^*(m, t)$ against the real one. Most papers report the relative NLL loss, that is, the average of the absolute difference between $-\log \hat{p}^*(m, t)$ and $-\log p^*(m, t)$ on the observed events (if markers are unavailable, $-\log \hat{p}^*(t)$ and $-\log p^*(t)$ [28, 33]). The lower relative NLL loss indicates a better performance. However, such a metric only evaluates performance at discrete events, which cannot gauge the overall discrepancy between $\hat{p}^*(m, t)$ and $p^*(m, t)$. So, this paper selects Spearman Coefficient ρ and L^1 distance to measure the discrepancy between $\hat{p}^*(m, t)$ and $p^*(m, t)$ over time, while we also report the relative NLL loss for reference.

Spearman Coefficient $\rho(X, Y)$ measures the relationship between two arbitrary value sequences, X and Y , as defined by Equation (32). If X and Y are more correlated, $\rho(X, Y)$ is higher; lower otherwise. Compared with the Pearson coefficient which is suitable if the relationship between X and Y is linear, Spearman coefficient could better deal with non-linear relationships. Because most probability distributions of TPP are non-linear, we select Spearman coefficient.

$$\rho(X, Y) = \frac{\text{Cov}(\text{Rank}(X), \text{Rank}(Y))}{\sigma_X \sigma_Y} \in [-1, 1] \quad (32)$$

where σ_X and σ_Y are the standard deviations of the values in sequence $X = \{x_1, x_2, \dots, x_n\}$ and $Y = \{y_1, y_2, \dots, y_n\}$, respectively. We expect ρ between $\hat{p}^*(m, t)$ and $p^*(m, t)$ is close to 1.

L^1 distance measures how different two arbitrary functions are in interval $[a, b]$.

$$L^1(f, g) = \int_a^b |f(x) - g(x)| dx \geq 0 \quad (33)$$

The smaller the L^1 distance is, the more similar $f(x)$ and $g(x)$ are. When $L^1(f, g) = 0$, $f(x)$ almost equals to $g(x)$ in interval $[a, b]$ for any $f(x)$ and $g(x)$, or $f(x) = g(x)$ at every $x \in [a, b]$ if both $f(x)$ and $g(x)$ are continuous.

D.3.2 Metrics for Real-World Datasets - macro-F1 & micro-F1

The macro-F1 value and micro-F1 value derives from the F1 value. F1 value has been widely used in almost all binary classification tasks because, compared with accuracy that might be fooled by false positives, F1 value takes accuracy and recall rate in its mind, where the model should correctly mark out positive samples for a better accuracy and negative samples for a better recall rate. The definition of F1 value is:

$$F1 = \frac{2 \times \text{Acc} \times \text{Recall}}{\text{Acc} + \text{Recall}} \quad (34)$$

F1 value is only for the binary classification. Some researchers realise that a multi-class classification can be evaluated by decomposing the original classification task into multiple binary classification tasks and averaging every obtained F1 values. This is how macro-F1 is devised. The expression of macro-F1 is:

$$\text{macro-F1} = \frac{1}{|M|} \sum_{m=1}^{|M|} F1_m \quad (35)$$

where $F1_m$ is the F1 value for marker m . macro-F1 treats all classes equally, so it has been widely used in studies addressing class imbalance.

On the other hand, micro-F1 is a global average of F1 values. Specifically, micro-F1 computes the sum of true positives, false negatives, and false positives over all classes then use Equation (34) to obtain the micro-F1. micro-F1 shows the overall performance regardless of the class.

If the mark prediction is based on $p^*(m)$ like our solution, macro-F1 and micro-F1 are independent of time prediction by nature. For baselines where mark prediction is based on $p^*(m|t)$, the mark involved in macro-F1 and micro-F1 is conditioned on the real time of the next event to ensure that macro-F1 and micro-F1 are independent of the time prediction. Specifically, for each real next event ($m = k_i, t'$) in a test set, we compute macro-F1 and micro-F1 using the mark predicted from $p(m|t')$.

D.3.3 Metrics for Real-World Datasets - Mean Absolute Error (MAE)

The test dataset T contains a subset of real next events. We denote $T_{m=k_i} \subset T$ as those real next events where the mark is $k_i \in M$. The number of events in $T_{m=k_i}$ is $|T_{m=k_i}|$. For each real next event $(m = k_i, t) \in T_{m=k_i}$, we are interested in the evaluation of time prediction. Consider all real next events in $T_{m=k_i}$, $\text{MAE}_{m=k_i}$ can be defined:

$$\text{MAE}_{m=k_i} = \frac{1}{|T_{m=k_i}|} \sum_{(m=k_i, t) \in T_{m=k_i}} |t - \bar{t}_{m=k_i}| \quad (36)$$

The absolute difference $|t - \bar{t}_{m=k_i}|$, between real time t and the predicted time $\bar{t}_{m=k_i}$ for mark k_i , is the prediction error for the real next event $(m = k_i, t)$. Here, k_i is not necessarily the predicted mark so that the time prediction evaluation is independent of mark prediction. MAE_{M_*} is the geometric mean of $\text{MAE}_{m=k_i}$ across all marks in M_* . M_* can be M , M_f , or M_r :

$$\text{MAE}_{M_*} = \sqrt[|M_*|]{\prod_{k_i \in M_*} \text{MAE}_{m=k_i}} \quad (37)$$

where $|M_*|$ is the number of marks in M_* .

D.4 Baselines

D.4.1 Group One

The first group of baselines includes: (i) *ours-w/o-thresholding*, which is the same as our method but the mark prediction is not optimized with thresholding. The mark prediction returns the mark with the highest mark probability as described in Section 2.1. The purpose is to evaluate the effectiveness of the thresholding method. (ii) *time-mark-with-thresholding*, that uses IFNMTPP to predict the time of the next event first, and then predicts the mark with the same thresholding method as *ours*. To do that, we predict time \bar{t} which is the mean of N samples from $p^*(t) = \sum_{m \in M} p^*(m, t)$ first, and then modify $p^*(m)$ in Equation (4) to $p^*(m|\bar{t})$ for mark prediction following the procedure described in Section 3.1. The purpose is to evaluate the necessity to predict mark first for handling mark imbalance with thresholding. (iii) *time-mark-w/o-thresholding*, is same as time-mark-with-thresholding but mark prediction is not optimized with thresholding.

D.4.2 Group Two

The second group of baselines evaluates thresholding against resampling, another classic technique to address data imbalance, including *undersampling* and *oversampling*. For undersampling, we reduce the frequency of other marks to ensure that they have the same number of training events as the rarest mark. For oversampling, we increase the frequency of other marks so that they have the same number of training events as the most frequent mark. For a fair comparison, the backbone MTPP method is IFNMTPP. After training completes for both baselines, the mark with the highest probability is predicted as the next event mark.

D.4.3 Group Three

The third group of baselines includes existing MTPP methods. Since MTPP modeling has been well studied in the past decades, the state-of-the-art methods demonstrate comparable performance. Among them, this study selects the most popular ones as baselines. Four neural MTPP methods based on conditional intensity function (CIF) are FullyNN [28], THP [44], SAHP [41], and AttNHP [26]. Besides these four, another baseline Marked-LNM [36] models $p^*(m)$ using a classifier to predict the mark of the next event and models $p^*(t|m)$ using LogNormMix to predict the time of the event.

- *Fully Neural Network(FullyNN)*[28] uses a neural network to estimate the integral of $\lambda^*(t)$ for the history embedding h and inter-event time t . Then the density function is formulated to predict the time of the next event. We rewrote FullyNN in PyTorch[30] based on the official implementation available at <https://github.com/omitakahiro/NeuralNetworkPointProcess>, which is publicly accessible without any license.

- *Transformer Hawkes Process(THP)*[44] uses a Transformer-based encoder to represent history as a hidden state \mathbf{h} . The softplus-based intensity function and the density function are modelled to predict the time of next event. We reproduce this model in PyTorch based on the paper.
- *Self-Attentive Hawkes Process(SAHP)*[41] is based on the same intuition as Continuous-time LSTM(CTLSTM)[24], which generalizes the classical Hawkes process by parameterizing its intensity function with recurrent neural networks. CTLSTM is an interpolated version of the standard LSTM, allowing us to generate outputs in a continuous-time domain. SAHP further improves performance by replacing LSTM with Transformers. Because the only difference between SAHP and CTLSTM is the history encoder, and SAHP has reported achieving better performance than CTLSTM, we only evaluate SAHP in this paper. We reproduce this model in PyTorch based on the paper.
- *AttNHP*[26] is another Transformer-based MTPP model. Different from THP and SAHP, where Transformer only encodes history, and the distribution is extracted from history representations using another deep module, AttNHP merges these two modules into one by directly extracting the distribution from historical events using a Transformer. We use the code provided by the author at <https://github.com/yangalan123/anhp-andtt>.
- *Marked LogNormMix(Marked-LNM)*[36] is an MTPP extension of the LogNormMix[33]. Marked-LNM also follows the MT paradigm by modeling $p^*(m)$ first, then using a composition of log Gaussian distribution to represent $p^*(t|m)$. To the best of our knowledge, Marked-LNM is the only MTPP approach predicting the mark of the next event first and then predicting the time of the event. However, Marked-LNM limits the form of $p^*(t|m)$ as the composition of log Gaussian distributions. This setting introduces inductive biases into the model, which could compromise the model prediction performance. We implement this model in PyTorch by modifying the official LogNormMix code at <https://github.com/shchur/ifl-tpp>. The official codes are released under the MIT license.

D.5 Data Preprocessing

We prepare synthetic and real-world datasets with normalization. For each dataset, normalization scales the time t of every event in each event sequence by the time mean \bar{t} of all events in all event sequences and standard deviation σ , as shown in Equation (38):

$$t_{scaled} = \frac{t - \bar{t}}{\sigma} \quad (38)$$

Normalization is useful when the time is relatively large, such as in the Retweet dataset. Table 8 shows how normalization is applied on various datasets.

Table 8: Data preprocessing.

Dataset	Retweet	StackOverflow	Taobao	USearthquake	five synthetic datasets
Normalization	✓	✓	✓	✓	✗

Our work focuses on predicting when the next event will happen provided a mark, especially a rare mark. For each dataset, we classify if one mark is rare or frequent. The percentages of marks in each dataset are presented in Figure 3. Table 9 shows which marks are classified as frequent and which are classified as rare.

Table 9: Rare marks and frequent marks.

Dataset name	The number of marks	Rare Mark	Frequent Mark
Retweet	3	[2]	[0, 1]
StackOverflow	22	[1, 2, 6, 7, 9, 10, 11, 12, 13, 14, 15, 16, 17, 18, 19, 20, 21]	[0, 3, 4, 5, 8]
Taobao	17	[0, 1, 2, 3, 4, 5, 6, 7, 8, 9, 10, 11, 12, 13, 14, 15]	[16]
USearthquake	7	[3, 4, 5, 6]	[0, 1, 2]

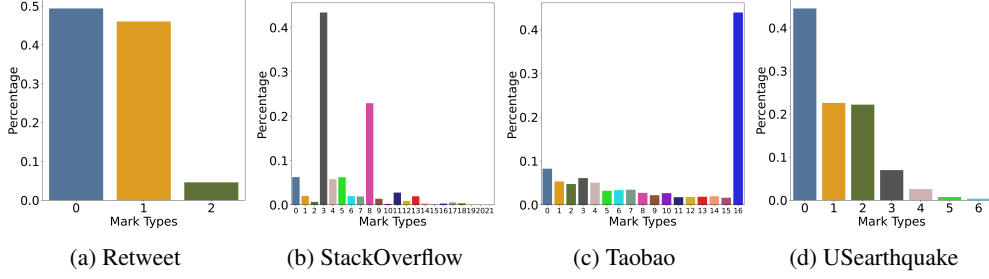


Figure 3: The frequency distribution of marks in real-world datasets.

D.6 Model Training

This section introduces the hyperparameter settings for all MTPP models used in this paper. The two values of “Steps” refer to the number of warm-up steps and total training steps, respectively. “BS” refers to batch size, and “LR” refers to the learning rate. Unless otherwise specified, we repeatedly train a model 3 times with different random seeds and report the mean and standard deviation of the results. We conduct all experiments on an internal cluster. It includes Intel Xeon CPUs and NVIDIA A100-PCIE GPUs. All codes will be released upon acceptance under the MIT license.

For each mark m , we sample N times $\{t^i\}_N^m$ from $F^*(t|m)$ to predict the time of the next event on the condition that its mark is m by the inverse transform sampling:

$$F^*(t^i|m) = u^i \quad (39)$$

where u^i is a random sample from a uniform distribution. The common practice samples u_i from the standard uniform distribution $u^i \sim \mathcal{U}(0, 1)$. MTPP allows t_i to go to positive infinity. When u^i is very close to 1, the time drawn from Equation (39) will be meaninglessly big and cause a negative impact to the accuracy of evaluation. To avoid this, we let $u^i \sim \mathcal{U}(0, 0.9)$. We find this trick can significantly stabilize the sampling process.

D.6.1 IFNMTPP Configurations

Table 10 lists the hyperparameter settings for IFNMTPP. The three values of “MS” (model structure) refer to the number of dimensions for history embedding \mathbf{h} , the number of dimensions for \mathbf{v}_m and \mathbf{b}_m ⁸, and the number of non-negative fully-connected layers in the IEM module, respectively.

Table 10: Hyperparameter settings for IFNMTPP.

Datasets	Steps	MS	BS	LR
Retweet	[80,000, 400,000]	[32, 16, 4]	32	0.002
Stackoverflow	[40,000, 200,000]	[32, 32, 2]	32	0.002
Taobao	[16,000, 80,000]	[32, 16, 4]	32	0.002
USearthquake	[40,000, 200,000]	[32, 16, 4]	32	0.002
Synthetic	[20,000, 100,000]	[32, 64, 3]	32	0.002

D.6.2 FullyNN Configurations

Table 11 shows hyperparameter settings for FullyNN. The three numbers in column “MS” share the same meaning as those in IFNMTPP.

D.6.3 THP Configurations

Table 12 shows all hyperparameter settings for THP. The six values of “MS” are the number of dimensions of the Transformer input vectors, the number of dimensions of the hidden outputs from an RNN which is on top of the Transformer encoder, the number of dimensions of the vectors used by self-attentions (q , k , and v), the number of Transformer layers, and heads.

⁸ \mathbf{v}_m and \mathbf{b}_m always have the same number of dimensions.

Table 11: Hyperparameter settings for FullyNN.

Datasets	Steps	MS	BS	LR
Retweet	[80,000, 400,000]	[32, 16, 4]	32	0.002
Stackoverflow	[40,000, 200,000]	[32, 32, 2]	32	0.002
Taobao	[16,000, 80,000]	[32, 16, 4]	32	0.002
USearquake	[40,000, 200,000]	[32, 16, 4]	32	0.002
Synthetic	[20,000, 100,000]	[32, 64, 3]	32	0.002

Table 12: Hyperparameter settings for THP.

Datasets	Steps	MS	BS	LR
Retweet	[80,000, 400,000]	[16, 16, 32, 8, 3, 3]	32	0.002
Stackoverflow	[40,000, 200,000]	[16, 16, 32, 8, 3, 3]	32	0.002
Taobao	[16,000, 80,000]	[16, 16, 32, 8, 3, 3]	32	0.002
USearquake	[40,000, 200,000]	[16, 16, 32, 8, 3, 3]	32	0.002
Synthetic	[20,000, 100,000]	[16, 32, 64, 16, 3, 4]	32	0.002

D.6.4 SAHP Configurations

The hyperparameter settings for SAHP are available in Table 13. The first six values of “MS” share the same meaning as those in THP while the last is the dropout rate.

Table 13: Hyperparameter settings for SAHP.

Datasets	Steps	MS	BS	LR
Retweet	[80,000, 400,000]	[16, 16, 32, 8, 3, 3, 0.1]	32	0.002
Stackoverflow	[40,000, 200,000]	[16, 16, 32, 8, 3, 3, 0.1]	32	0.002
Taobao	[16,000, 80,000]	[16, 16, 32, 8, 3, 3, 0.1]	32	0.002
USearquake	[40,000, 200,000]	[16, 16, 32, 8, 3, 3, 0.1]	32	0.002
Synthetic	[20,000, 100,000]	[16, 32, 64, 16, 3, 4, 0.1]	32	0.002

D.6.5 AttNHP Configurations

The hyperparameter settings for AttNHP are available in Table 14. The first six values of “MS” share the same meaning as those in THP while the last is the dropout rate.

Table 14: Hyperparameter settings for SAHP.

Datasets	Steps	MS	BS	LR
Retweet	[80,000, 400,000]	[16, 16, 64, 8, 3, 3, 0.0]	32	0.002
Stackoverflow	[40,000, 200,000]	[16, 16, 64, 8, 3, 3, 0.0]	4	0.002
Taobao	[16,000, 80,000]	[16, 16, 64, 8, 3, 3, 0.0]	32	0.002
USearquake	[40,000, 200,000]	[16, 16, 64, 8, 3, 3, 0.0]	32	0.002
Synthetic	[20,000, 100,000]	[16, 16, 64, 8, 3, 3, 0.0]	32	0.002

D.6.6 Marked-LNM Configurations

The hyperparameter settings for Marked-LNM are presented in Table 15. The three values of “MS” are the number of the dimensions of LSTM, the number of the dimensions of mark embedding, and the number of Gaussian distributions, respectively.

E Additional Experiment Results

E.1 Performance of IFNMTPP for modeling $p^*(m, t)$

For a better and integration-free solution, IFNMTPP models the improper integration of $p^*(m, t)$. The advantage has been verified by the experiment results reported in Table 6. IFNMTPP models

Table 15: Hyperparameter settings for Marked-LNM.

Datasets	Steps	MS	BS	LR
Retweet	[80,000, 400,000]	[32, 32, 16]	32	0.002
Stackoverflow	[40,000, 200,000]	[32, 32, 16]	32	0.002
Taobao	[16,000, 80,000]	[32, 32, 16]	32	0.002
USearhquake	[40,000, 200,000]	[32, 32, 16]	32	0.002
Synthetic	[20,000, 100,000]	[32, 32, 16]	32	0.002

$p^*(m, t)$ at the same time while modeling the improper integration of $p^*(m, t)$. Compared to other existing MTPP models, the performance of IFNMTPP in modeling $p^*(m, t)$ is evaluated and reported in Table 16. The evaluation metric is NLL loss, the average of the $-\log p^*(m, t)$ at the observed events. The lower NLL loss indicates a better performance. We can observe that IFNMTPP shows a competent performance.

Table 16: Accuracy of $p^*(m, t)$ measured by NLL loss on real-world datasets. Lower is better.

	IFNMTPP (Ours)	FullyNN	SAHP	THP	AttNHP	Marked-LNM
Retweet	6.3225 ± 0.0007	6.6437 ± 0.0380	6.1935 ± 0.0184	10.379 ± 0.5349	6.0084 ± 0.0086	6.5292 ± 0.0064
Stackoverflow	2.0540 ± 0.0029	3.6984 ± 0.0022	2.0713 ± 0.0028	2.5565 ± 0.0216	2.0811 ± 0.0054	2.0992 ± 0.0014
Taobao	-0.7762 ± 0.0565	-0.0431 ± 0.0484	-1.2779 ± 0.0421	140.91 ± 81.166	-1.2190 ± 0.0763	1.2720 ± 0.1300
USearhquake	1.3278 ± 0.0533	1.8664 ± 0.0649	1.3544 ± 0.0300	2.0744 ± 0.3174	1.4120 ± 0.0499	1.8514 ± 0.0462

E.2 Evaluating Model Fidelity on Synthetic datasets

In this section, we report the full result of model fidelity test on synthetic datasets involving IFNMTPP and other baselines. The IFNMTPP consistently learns more accurate $p^*(m, t)$ than other baselines as supported by the lower L^1 distance and higher Spearman coefficient. These findings suggest that predictions based on IFNMTPP should be more reliable and accurate.

Table 17: Model fidelity test performance on synthetic datasets; higher Spearman, lower L^1 and relative NLL loss are better; the bold and underline indicate the best and the second-best values, respectively.

		Hawkes_1	Hawkes_2	Poisson	Self-correct	Stationary Renewal
Spearman	IFNMTPP (Ours)	1.0000 ± 0.0000	0.9999 ± 0.0000	1.0000 ± 0.0000	0.9551 ± 0.0009	0.9999 ± 0.0000
	FullyNN	0.9952 ± 0.0004	0.9963 ± 0.0002	0.9722 ± 0.0018	0.9477 ± 0.0001	0.9998 ± 0.0000
	SAHP	0.9959 ± 0.0047	0.9862 ± 0.0000	0.9615 ± 0.0025	0.9492 ± 0.0014	0.9990 ± 0.0007
	THP	0.9266 ± 0.0026	0.7366 ± 0.0005	1.0000 ± 0.0000	0.6969 ± 0.0017	0.0413 ± 0.0024
	AttNHP	-	-	-	-	-
	Marked-LNM	0.9924 ± 0.0007	0.9971 ± 0.0001	0.9713 ± 0.0024	0.9491 ± 0.0005	0.9999 ± 0.0000
L^1	IFNMTPP (Ours)	0.1480 ± 0.0085	0.3105 ± 0.0432	0.0133 ± 0.0091	0.5163 ± 0.0290	0.0654 ± 0.0018
	FullyNN	0.6235 ± 0.0227	3.1048 ± 0.0763	0.2973 ± 0.0098	1.1889 ± 0.0244	0.0710 ± 0.0099
	SAHP	1.0245 ± 0.2967	4.7867 ± 0.2735	0.6893 ± 0.0238	1.3363 ± 0.0196	0.4872 ± 0.1833
	THP	12.003 ± 0.2069	25.500 ± 0.3642	<u>0.0203 ± 0.0067</u>	10.656 ± 0.0965	9.9230 ± 0.0451
	AttNHP	-	-	-	-	-
	Marked-LNM	0.6994 ± 0.0117	2.6446 ± 0.0633	0.3620 ± 0.0044	0.7406 ± 0.0168	0.0402 ± 0.0001
Relative NLL	IFNMTPP (Ours)	0.0000 ± 0.0000	0.0001 ± 0.0000	0.0000 ± 0.0000	0.0007 ± 0.0003	0.0000 ± 0.0000
	FullyNN	0.0003 ± 0.0000	0.0008 ± 0.0001	0.0002 ± 0.0000	0.0015 ± 0.0001	0.0000 ± 0.0000
	SAHP	0.0086 ± 0.0017	0.0312 ± 0.0193	0.0092 ± 0.0002	0.0072 ± 0.0009	0.0034 ± 0.0010
	THP	0.2137 ± 0.0001	0.6663 ± 0.0029	0.0000 ± 0.0000	0.1262 ± 0.0004	0.0771 ± 0.0000
	AttNHP	0.8202 ± 0.0053	0.0387 ± 0.0144	0.2631 ± 0.0009	0.0820 ± 0.0003	0.3065 ± 0.0007
	Marked-LNM	0.0004 ± 0.0000	0.0010 ± 0.0000	0.0006 ± 0.0000	0.0018 ± 0.0001	0.0000 ± 0.0000

E.3 Comparing IFNMTPP with Marked-LNM and thresholding

Among all baselines, only Marked-LNM follows the mark-time modeling paradigm and is suitable with thresholding. We therefore compare the mark prediction accuracy of our method and Marked-LNM under thresholding. The results, summarized in the table below, demonstrate that our method outperforms Marked-LNM in mark prediction. Note that we do not report time prediction results for this comparison, as the time prediction is unaffected by the method used for predicting marks. Nonetheless, as shown in Table 6, our method also achieves strong performance in time prediction.

Table 18: Comparison of IFNMTPP with Lognormmix + thresholding on four data sets, measured by macro-F1/micro-F1. The bold are the best values.

		Retweet	SO	Taobao	USearthquake
ours	M	0.4750±0.0033 / 0.4394±0.0093	0.1776±0.0030 / 0.6376±0.0026	0.4190±0.0104 / 0.7499±0.0151	0.1382±0.0071 / 0.3189±0.0125
	M_r	0.2010±0.0082 / 0.2010±0.0082	0.1476±0.0041 / 0.4530±0.0026	0.3987±0.0108 / 0.7558±0.0185	0.0339±0.0051 / 0.1111±0.0098
	M_f	0.6120±0.0013 / 0.9612±0.0021	0.2795±0.0014 / 0.8974±0.0042	0.7441±0.0060 / 0.7441±0.0060	0.2773±0.0215 / 0.9181±0.0102
Marked-LNM + thresholding	M	0.4228±0.0014 / 0.3876±0.0093	0.1121±0.0007 / 0.4469±0.0124	0.1558±0.0623 / 0.7945±0.0060	0.1198±0.0078 / 0.3438±0.0035
	M_r	0.1730±0.0033 / 0.1730±0.0033	0.1004±0.0004 / 0.3527±0.0065	0.1181±0.0653 / 0.8318±0.0019	0.0393±0.0004 / 0.1740±0.0074
	M_f	0.5477±0.0004 / 0.8687±0.0005	0.1519±0.0017 / 0.5662±0.0209	0.7589±0.0133 / 0.7589±0.0133	0.2271±0.0169 / 0.6810±0.0427